131

1518

AD A133 467

R and D CENTER
LABORATORY
TECHNICAL REPORT

NO. 12688

DESIGN AND MICROPROCESSOR-BASED IMPLEMENTATION OF DIGITAL FREQUENCY SELECTIVE FILTERS FOR APPLICATION IN TERRAIN ROUGHNESS IDENTIFICATION

U.S. ARMY TACOM

by K.C. Cheok and N.K. Loh

Center for Robotics and Advanced Automation
School of Engineering
Oakland University
Rochester, Michigan 48063

Contract DAAE07-81-C-4058

APPROVED FOR PUBLIC RELEASE:
DISTRIBUTION UNLIMITED

U.S. ARMY TANK-AUTOMOTIVE COMMAND
RESEARCH AND DEVELOPMENT CENTER
Warren, Michigan 48090

1621

NOTICES

REPORT DOCUMENTATION PAGE		READ INSTRUCTIONS BEFORE COMPLETING FORM
1. REPORT NUMBER 12688	2. GOVT ACCESSION NO.	3. RECIPIENT'S CATALOG NUMBER
4. TITLE (and Subtitle) Design and Microprocessor-Based Implementation of Digital Frequency Selective Filters for Application in Terrain Roughness Identification.		5. TYPE OF REPORT & PERIOD COVERED Interim July 81 to April 82 6. PERFORMING ORG. REPORT NUMBER TR-82-04-121
7. AUTHOR(s) Dr. K.C. Cheok and Dr. N.K. Loh		8. CONTRACT OR GRANT NUMBER(s) DAAE07-81-C-4058
9. PERFORMING ORGANIZATION NAME AND ADDRESS School of Engineering Oakland University Rochester, MI 48063		10. PROGRAM ELEMENT, PROJECT, TASK AREA & WORK UNIT NUMBERS
11. CONTROLLING OFFICE NAME AND ADDRESS DRSTA-RCKT U.S. ARMY TACOM Warren, MI 48090		12. REPORT DATE April 1982 13. NUMBER OF PAGES 98
14. MONITORING AGENCY NAME & ADDRESS(if different from Controlling Office) DRSTA-ZSA U.S. ARMY TACOM Warren, MI 48090		15. SECURITY CLASS. (of this report) Unclassified 15a. DECLASSIFICATION/DOWNGRADING SCHEDULE N/A
16. DISTRIBUTION STATEMENT (of this Report) Approved for public release: Distribution Unlimited.		
17. DISTRIBUTION STATEMENT (of the abstract entered in Block 20, if different from Report)		
18. SUPPLEMENTARY NOTES		
19. KEY WORDS (Continue on reverse side if necessary and identify by block number) Microprocessors, Surface Roughness, Frequency Bands, Digital Recursive Filters, Highpass Filters, Lowpass Filters, Bandpass Filters.		

20. ABSTRACT (Continue on reverse side if necessary and identify by block number)

The design and implementation of microprocessor-based frequency selective filters for possible use in an on-board terrain roughness identification scheme are investigated. In the design aspect of the investigation, a systematic digital filter design procedure is developed. The effectiveness of the procedure is illustrated by several digital filter design examples. In the implementation aspect, a digital signal processing firmware (hardware and software) based on the Motorola 6802 microprocessor is developed. The

microprocessor realization of the exemplary digital filters are carried out. Actual experimental results are recorded and compared to their theoretical simulations. The capability of the firmware which includes the computational speed and numerical accuracies will be shown to be adequate for the present purpose.

PREFACE

Technical advances in the on-the-move adjustability of military vehicle suspension components, on board terrain sensing, modern system control theory, and microprocessors have combined in recent years to greatly increase the potential for improving the ride performance of military vehicles. Increasing emphasis on fire-on-the move, lighter weight combat vehicles, and higher horsepower per ton ratios make the role of the suspension system more critical for mission performance. This report documents and develops the theory and methods required for real time processing of sensed terrain elevation data in order to make it useful for suspension adjustment decisions. It also demonstrates the successful real time application of the techniques on a currently available microprocessor.

This work was performed for the Tank-Automotive Systems Laboratory of the U.S. Army Tank-Automotive Command, Warren, Michigan, under the overall direction of Mr. Michael Kaifesh, Chief of the Track and Suspension sub-function, and Mr. Leonard Sloncz, Track and Suspension project engineer. Mr. Robert Daigle of the Applied Research Function was technical monitor for the contract.

THIS PAGE LEFT BLANK INTENTIONALLY

TABLE OF CONTENTS

THIS PAGE LEFT BLANK INTENTIONALLY

LIST OF ILLUSTRATIONS

LIST OF TABLES

1.0 INTRODUCTION

The possibility of obtaining improvement in the ride quality of a vehicle using a damping rate which varies according to the terrain roughness has been considered in literatures such as [1] - [5]. Recently, a preliminary feasibility study on the identification of terrain roughness and frequency characteristics was carried out by Daigle [5] using sampled-data analysis and digital filtering techniques. In this study, a mathematical decision scheme for characterizing the terrain roughness in terms of its frequency (wave lengths) contents is developed. The development assumes that the terrain elevation can be sensed, sampled and digitized . The terrain elevation sampled-data stream is then passed through frequency selective filters which separate the frequency components of the data into different adjacent bands or channels on the frequency spectrum. The RMS value from each channel is computed, and the relative amplitude of the RMS values is used to indicate certain degrees of terrain roughness present in each of the channels.

Simulations of the above sampled-data, digital filtering and decision scheme were made on the Systems Engineering Laboratories (SEL) digital computer. The effectiveness of the scheme for indicating or identifying the terrain roughness was strongly supported by the simulation results. The use of the terrain roughness identification scheme is proposed [5], among other techniques, as a possible means of incorporating a microprocessor-based on-board adaptive suspension control unit for a vehicle.

To determine the feasibility of an actual implementation of the microprocessor-based on-board system, a preliminary investigation into experimental microprocessor-based filters is suggested. A main concern of the investigation is the computational speed and numerical accuracies of the microprocessor in the realization of high order digital filters. As a rough guideline, it is noted that the digital frequency selective filters used in the formulation of the above terrain roughness identification scheme consist of bandpass and highpass filters whose critical frequencies are less than 10 Hz.

2.0 OBJECTIVES

The objective of this report is to investigate the design and to carry out the actual implementation of microprocessor-based frequency selective filters which may be suitable for the terrain roughness identification purposes. In the design phase of the investigation, a systematic procedure for designing digital filters is developed. The procedure is based on bilinear transformation technique with emphasized consideration on the compensation of frequency warping and on the choice of the ratio of working frequency to sampling frequency. The effectiveness of the proposed design procedure will be demonstrated by several examples. It is remarked that the potential of the procedure may be enhanced by the incorporation of computer-aided digital filter design techniques.

In the implementation phase of the investigation, the hardware and software for a microprocessor-based digital signal processing system will be developed. Microprocessor realization of digital frequency selective filters will be demonstrated by the implementation of digital lowpass, highpass, bandpass and bandstop filters. The actual experimental frequency responses of the microprocessor-based digital filters will be recorded and compared to their theoretical frequency responses.

The organization of this report is as follows. The systematic procedure for the design of digital filters is developed in Section 5.1, the hardware and software for the microprocessor-based signal processing system and filters is described in Section 5.2 and Appendix B. The actual experimental frequency response of the microprocessor-based digital filters is given in Section 5.3. Section 4 discusses the results of the investigation and provides a few recommendations for the direction of future effort. A summary on the design of analog Butterworth frequency selective filters is given in Appendix A.

THIS PAGE LEFT BLANK INTENTIONALLY

3.0 CONCLUSIONS

The design procedure developed in Section 5 provides a systematic technique for obtaining a digital filter from a corresponding analog filter using bilinear transformation. The technique takes into consideration the frequency warping and the ratio of working to sampling frequencies. The effectiveness of the design procedures is illustrated by Examples 1 - 5, where the design specifications are satisfactorily fulfilled.

Based on the experimental results and performance of the microprocessor-based frequency selective filters presented in Section 5, the following may be inferred:

- The computational speed of the microprocessor-based system is sufficiently fast for the implementation of the digital frequency selective filters with the required specifications. As noted in the Introduction, the critical frequencies of the digital filters required in the terrain roughness identification schemes are less than 10 Hz. It is seen in Table 2 that the critical frequencies of the experimental microprocessor-based filters can be much higher than the required specification.* This further implies that there is room in the processing time for implementing higher order filters.
- The numerical accuracies of the microprocessor-based system using 12-bit word length data is adequate for the implementation of the filters. This is clearly illustrated by comparing the theoretical frequency responses of the digital filters depicted in Figs. 6, 8, 10, 12 and 14 to the actual experimental frequency responses of the microprocessor-based filters depicted by Figs. 19, 20, 21, 22 and 23.

---

* It is reminded that the microprocessor-based filters can readily be tuned, by adjusting the sampling frequency ω_s, so that the critical frequencies coincide with the desired specifications.

THIS PAGE LEFT BLANK INTENTIONALLY

4.0 RECOMMENDATIONS

The successful preliminary investigation into the microprocessor realization of the digital frequency selective filters provides a favorable possibility for implementing a microprocessor-based on-board terrain roughness identification system using digital filtering techniques. The following effort in line with the investigation of microprocessor-based signal processing system in this report may be pursued in the future:

- Implementation of microprocessor-based system with parallel processing;
- Use of 16-bit microprocessors;
- Use of fast arithmetic and support chips;
- Computer aided design package for the design procedures developed in Section 5
- Implementation of the mathematical decision criterion for identifying the terrain roughness and frequency content as suggested in [5].

Some of these efforts are currently underway.

THIS PAGE LEFT BLANK INTENTIONALLY

5.0 DISCUSSION

5.1 DESIGN OF DIGITAL FILTERS

The basic steps in the design of digital filters generally involve:

(i) the specification on the general characteristics of the filters;
(ii) the approximation and design consideration in attaining the specification;
(iii) the realization of the filters using finite precision arithmetic.

Step (i) depends mainly on the application of the filters while step (ii) depends on the design approach adopted by the designer. Step (iii) takes into account the limitations of digital devices, such as the finite word length in a digital circuit or machine and the finite computational speed.

The objective of this section is concerned with step (ii) of the design; step (iii) will be considered in the next section. In particular, the design of infinite impulse response (IIR) digital filters (lowpass, highpass, bandpass and bandstop filters) using analog filter formulas and bilinear transformation will be presented in detail in this section.

While a digital filter may directly be designed using pole-zero placement technique in the z-plane, a more traditional approach is to transform an analog filter, based on the poles and zeroes in the s-plane, into a corresponding digital filter satisfying a prescribed specification. Some of the reasons for the latter approach include :

- the straightforward convergence of frequency specification (in terms of Hz or rad-s^{-1}) for an analog filter into the frequency specification (in terms of radian frequency, angle around the unit circle, or ratio of frequencies) for the digital filter, once the sampling rate is given;
- the utilization of the highly developed art in the design of a variety of analog filters to obtain the corresponding digital filters (e.g. Butterworth, Chebychev or elliptic filters)
- the closed-form design formulas for analog filters which can be translated

to yield closed-form design formulas for the corresponding digital filters. The closed-form formulas facilitate simplicity in the realization of the filters.

There are many techniques for transforming or converting an analog filter into a corresponding digital filter. One such technique is the bilinear transformation which is described below.

5.1.1 DESIGNING DIGITAL FILTERS FROM ANALOG FILTERS USING BILINEAR TRANSFORMATION WITH WORKING TO SAMPLING FREQUENCY RATIO CONSIDERATION

The design of digital filters from application of bilinear transformation to the formulas of analog filters has been considered in literature such as [6]-[7]. Most of the design procedures in these literature, however, do not include a systematic way for determining the gain(say, τ) in the bilinear transformation. As will be seen shortly, the transformation gain τ is closely related to the quality in the zero-order-hold reproduction of a processed sampled data from an analog signal by a digital filter. To ensure a desirable reproduction quality in the digital filter output, it is important that a proper transformation gain is used in the design.

In this section, we present a systematic approach to the design of digital filters from analog filters using the bilinear transformation which takes the ratio of working or critical frequencies of the digital filter to the sampling frequency into the design consideration. The approach provides a straightforward procedure for choosing the transformation gain τ and for obtaining the desirable output reproduction quality in the digital filter. The procedure is also well suited for use in computer-aided digital filter designs.

BILINEAR TRANSFORMATION

For sampled-data signals, the Laplace transform (s-transform) can be shown to be related to the z-transform by

$$z = e^{sT} \quad , \tag{1}$$

where T is the sampling period. Using Pade's approximation [8], (1) can be approximated by

$$e^{sT} \simeq \frac{1 + sT/2}{1 - sT/2} \quad . \tag{2}$$

In general, one may redefine the mapping as

$$z \triangleq \frac{1 + s\tau/2}{1 - s\tau/2} \tag{3a}$$

or

$$s = \frac{2}{\tau} \frac{z - 1}{z + 1}, \tag{3b}$$

where τ is the transformation gain. Relationship (3) is known as BILINEAR TRANSFORMATION.

The mapping of the s-plane into the z-plane by bilinear transformation (s) is shown in Fig. 1, which can be constructed using the following relationships.

Define (see also Fig. 1)

$\omega_a \triangleq$ analog frequency (rad-s^{-1}),
$\omega_d \triangleq$ corresponding digital frequency (rad-s^{-1}),
$\omega_s \triangleq 2\pi/T$ = sampling frequency (rad-s^{-1}),

$\theta \triangleq \frac{\omega_d}{\omega_s} 2\pi = \omega_d T$ = radian frequency (rad).

(a) Using (3a), the frequency axis of the s-plane (the imaginary axis, $s = j\omega_a$) is mapped into that of the z-plane (the unit circle, $z = e^{j\theta}$) as follows:

$$z = \left. \frac{1 + s\tau/2}{1 - s\tau/2} \right|_{s=j\omega_a}$$

$$= \frac{1 + j\omega_a\tau/2}{1 - j\omega_a\tau/2}$$

$$= \frac{\sqrt{[1 + (\omega_a\tau/2)^2]}\, e^{j\tan^{-1}(\omega_a\tau/2)}}{\sqrt{[1 + (\omega_a\tau/2)^2]}\, e^{j\tan^{-1}(-\omega_a\tau/2)}}$$

$$= e^{j2\tan^{-1}(\omega_a \tau/2)}$$

$$\triangleq e^{j\theta} \tag{4}$$

Since $\theta = \frac{\omega_d}{\omega_s} 2\pi = \omega_d T$, (4) yields

$$\omega_d T = 2\tan^{-1}(\omega_a \tau/2) \tag{5a}$$

or

$$\omega_a = \frac{2}{\tau} \tan\left(\frac{\omega_d}{\omega_s} \pi\right) . \tag{5b}$$

The relationship (5) represents the frequency warping or distortion of bilinear transformation. The characteristic of the distortion is depicted in Figs. 2 and 3.

(b) From (3a), the real axis ($s = \sigma$) of the s-plane is mapped into the z-plane as the magnitude of

$$z = \frac{1 + \sigma\tau/2}{1 - \sigma\tau/2} , \tag{6}$$

where σ is real, and where it is seen that

$$-1 < z < 1 \text{ for } -\infty < \sigma < 0$$

$$1 \leq z < \infty \text{ for } 0 \leq \sigma < 2/\tau$$

$$-\infty < z < -1 \text{ for } \frac{2}{\tau} < \sigma < \infty .$$

It is clear from the above that the left half of the s-plane is mapped into the unit disk of the z-plane.

Now, let G(s) denote the transfer function of an analog filter and G(z) denote that of a corresponding digital filter. Then using bilinear transformation (3), the digital filter can be obtained as

$$G(z) = G(s) \Big|_{s = \frac{2}{\tau}\frac{z-1}{z+1}} \quad . \tag{7}$$

By the mapping of the bilinear transformation (Fig. 1), all the stable poles of G(s) will be converted into stable poles in G(z). Consequently, the bilinear transformation (7) always yield stable digital filters from stable analog filters.

The effect of frequency warping or distortion (5) on the analog to digital filter conversion (7) is illustrated in Fig. 3. The figure also clearly reveals an explanation for the phenomenon of aliasings.

It is remarked that the transformation gain τ for the bilinear transformation (7) has not been specified. A systematic technique for determining τ is given in the sequel. The technique also automatically compensates for the frequency warping or distortion.

DESIGN CONSIDERATION

The digital zero-order-hold (ZOH) reproduction of an analog signal having a dominant working frequency ω_a (or correspondingly ω_d) depends on the ratio ω_d/ω_s. Fig. 4 illustrates the variation, with respect to the ratio ω_d/ω_s, by a sample and ZOH scheme.[1] As can be seen from the figure, the "quality" of the digital reproduction of the analog signal improves with lower ratio of ω_d/ω_s. It is, therefore, desirable to design a digital filter whose working or critical frequencies are much lower than the sampling frequencies. A first design consideration in a digital filter design is to ensure that the ratio

$$0 < \omega_d/\omega_s << .5 \quad . \tag{8}$$

[1] The microproessor-based sample and ZOH scheme is described in Section 3.

Remark 1: For simplicity and clarity, the above argument is approached from time-domain point of view using visual experimental results. It may be remarked that similar conclusions can be obtained using frequency domain analysis [6]. One also notes that (8) is in agreement to the Sampling Theorem due to Shannon and Nyquist [6].

It is also important to observe the time delays in the digital outputs in reference to the continuous signals in Fig. 4.

Δ

Once the ratio ω_d/ω_s has been selected, one may define a factor R as

$$R \triangleq \tan\left(\frac{\omega_d}{\omega_s}\pi\right), \qquad 0 < \omega_d/\omega_s < .5$$

$$= \frac{\omega_a \tau}{2}, \tag{9}$$

where (9) follows from (5). Note that $0 < R < \infty$. From (9), the transformation gain τ is obtained as

$$\tau = \frac{2R}{\omega_a}. \tag{10}$$

Using (8) in (3b), the bilinear transformation becomes

$$s = \frac{\omega_a}{R}\,\frac{z-1}{z+1}. \tag{11}$$

The above design consideration of first specifying a desired ratio ω_d/ω_s thus leads to a systematic choice of the transformation gain τ for the bilinear transformation as shown in (11).

Using (11) as the basis for bilinear transformation, the conversion of an analog filter G(s) with working or critical frequency ω_a to a corresponding digital filter G(z) with working or critical frequency ω_d, follows from (7) as

$$G(z) = G(s) \Big|_{s = \frac{\omega_a}{R} \frac{z-1}{z+1}} \quad . \tag{12}$$

The bilinear transformation in (12) ensures that the desired ω_d/ω_s will be obtained.

Finally, it is important to note that the working or critical frequency ω_d of the digital filter can be varied by simply adjusting the sampling frequency ω_s.

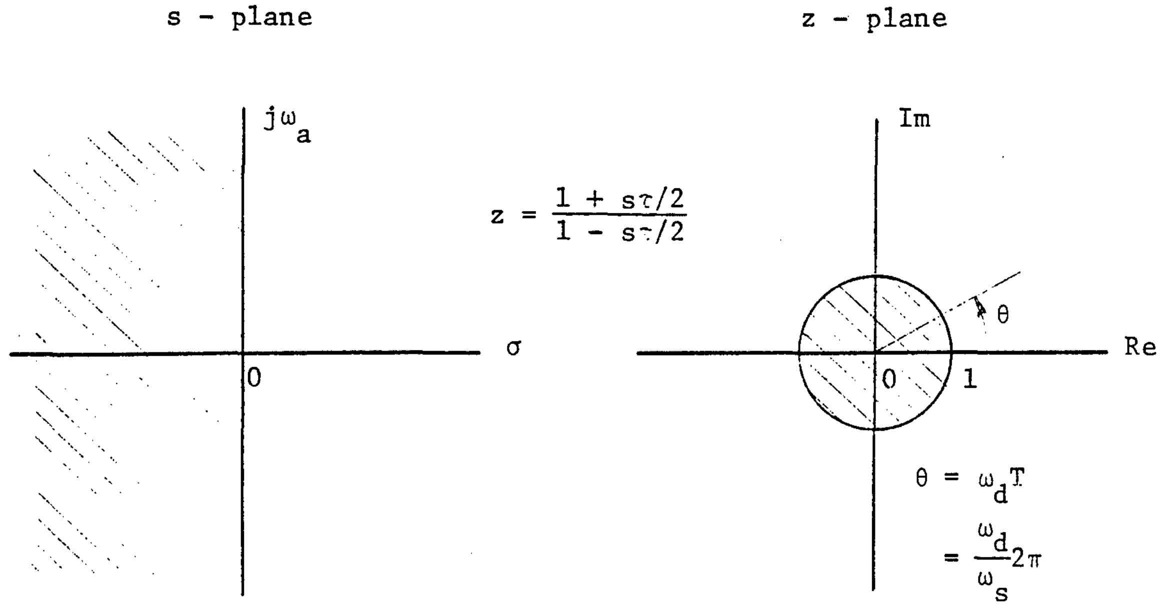

Fig. 1. Mapping of s - plane into z - plane by bilinear transformation

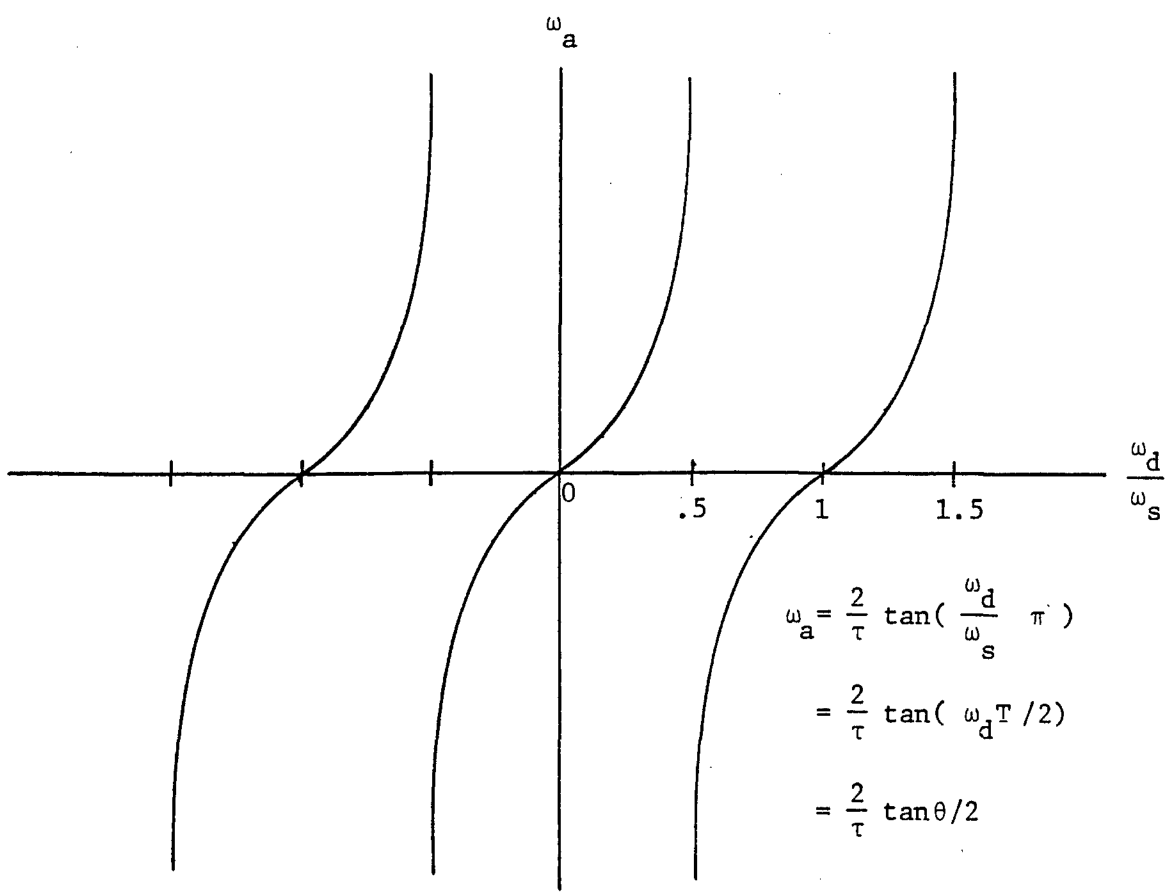

Fig. 2. Frequency warping in bilinear transformation

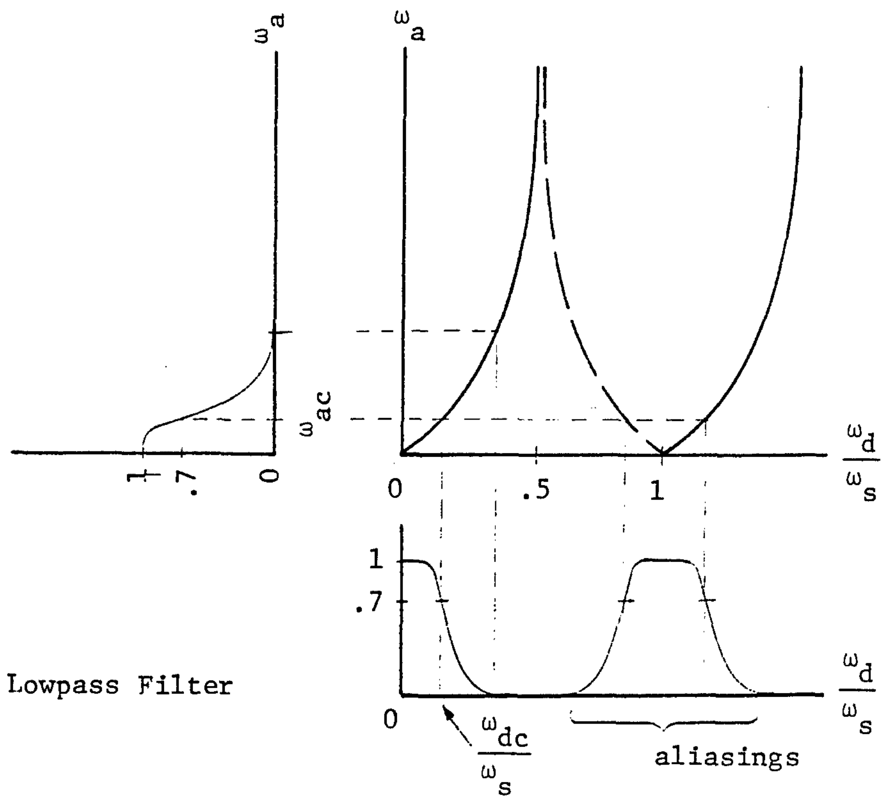

Fig. 3a) Lowpass Filter

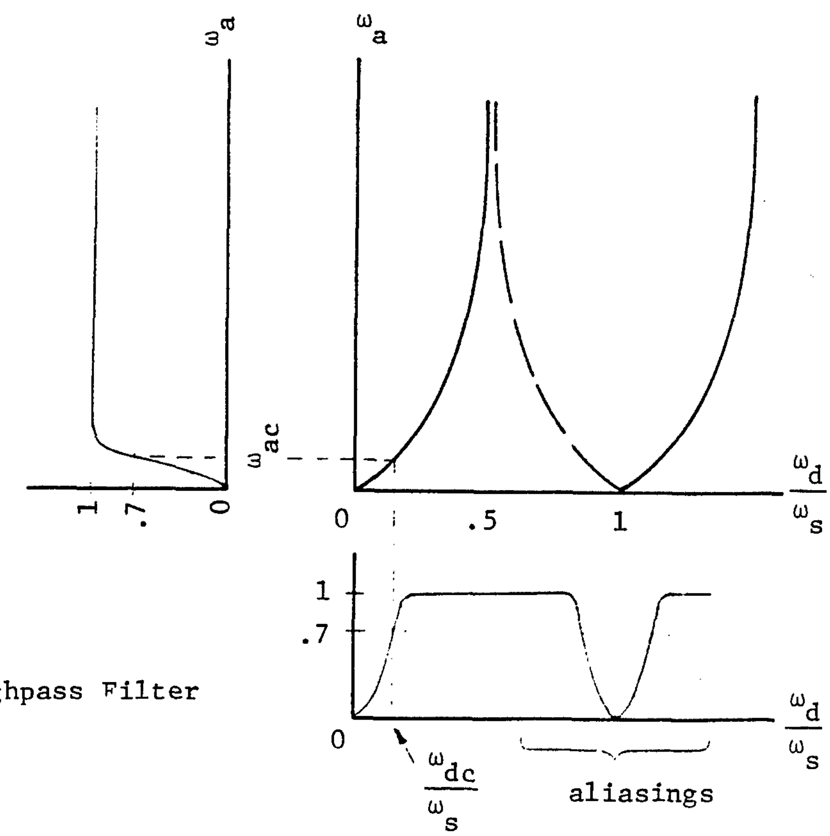

Fig. 3b) Highpass Filter

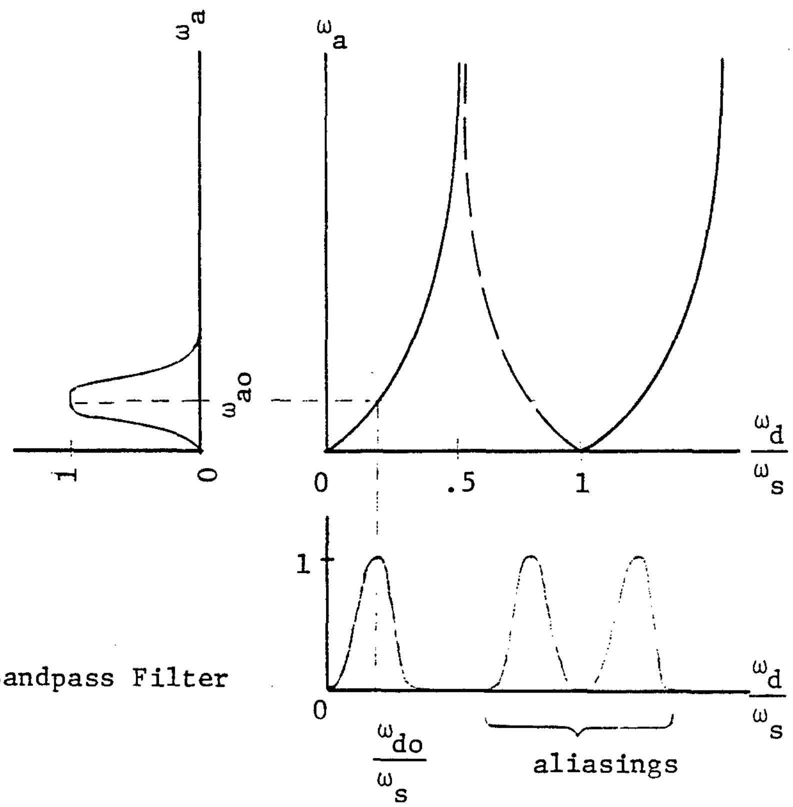

Fig. 3c) Bandpass Filter

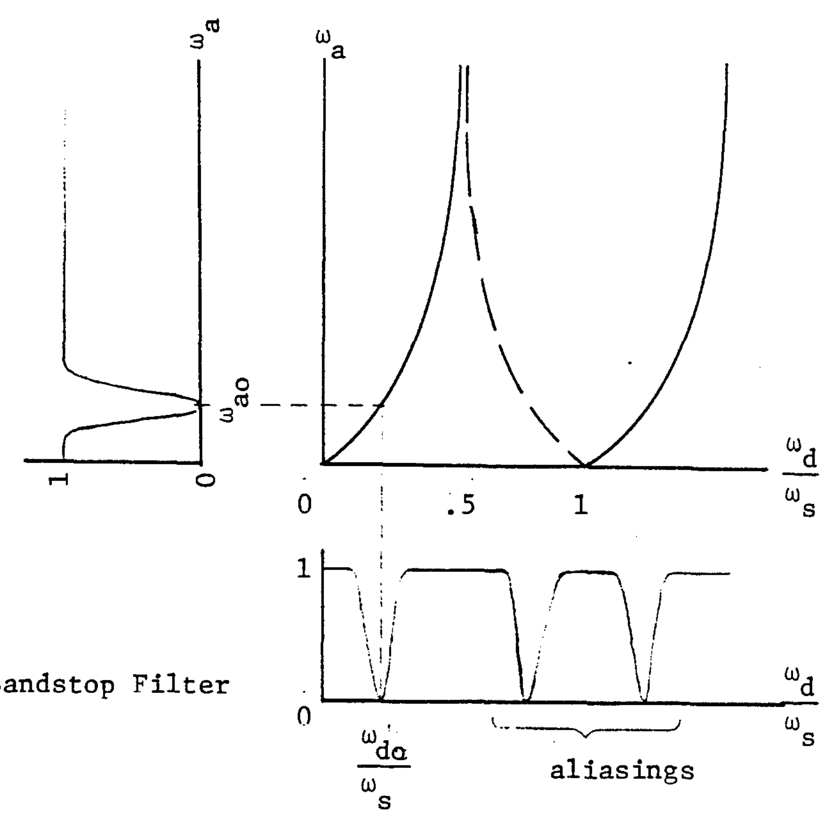

Fig. 3d) Bandstop Filter

Fig. 3 Effects of Frequency Warping on Frequency Selective Filters

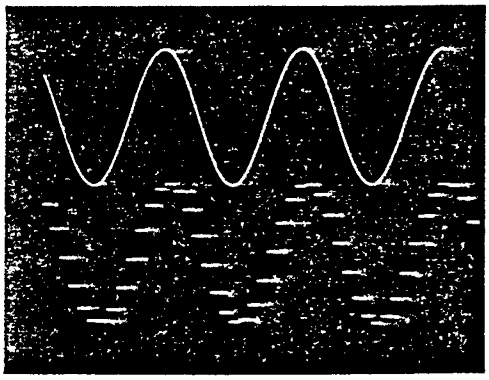

$\omega_d/\omega_s = 1/15$

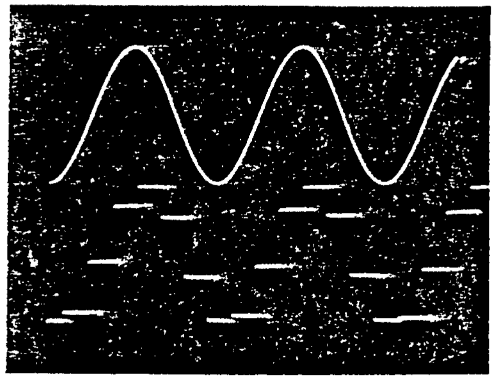

$\omega_d/\omega_s = 1/7$

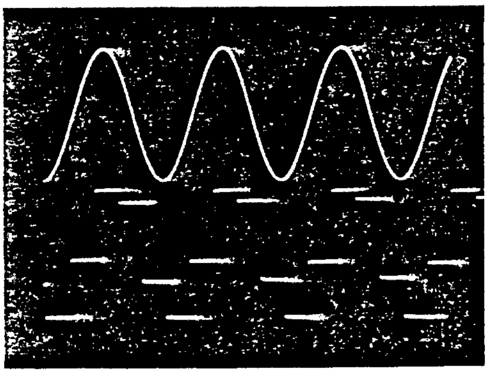

$\omega_d/\omega_s = 1/5$

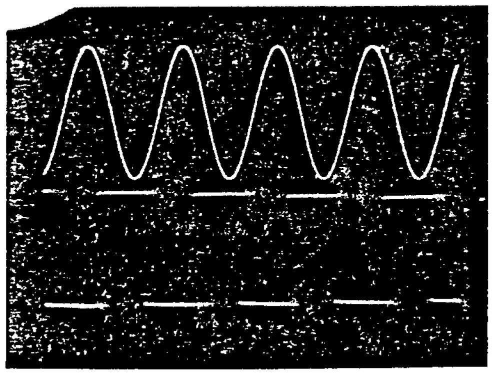

$\omega_d/\omega_s = 1/2$

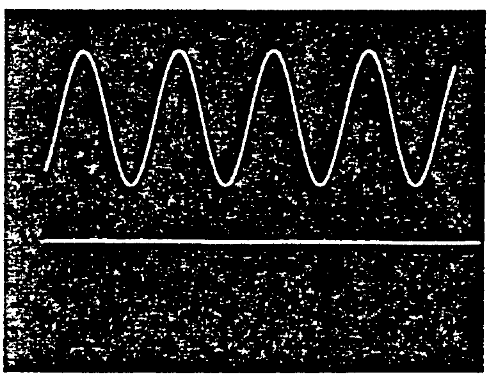

$\omega_d/\omega_s = 1$

Fig.4. ZOH Reproduction of Sinusoidal Signal with respect to Ratio ω_d/ω_s.

5.1.2 DESIGN OF DIGITAL LOWPASS FILTERS

The design of an n-th order analog Butterworth lowpass filter $G_{LP}(s)$ with critical cut-off frequency ω_{ac} is given in Appendix A2. To obtain a corresponding digital Butterworth lowpass filter $G_{LP}(z)$, the following systematic procedure may be used:

(a) Select the ratio ω_{dc}/ω_s, where ω_{dc} is the desired critical cut-off frequency of the digital lowpass filter (see Fig.3a).

(b) Obtain the factor R and transformation gain as

$$R = \tan\left(\frac{\omega_{dc}}{\omega_s}\pi\right)$$

$$= \frac{\omega_{ac}\tau}{2} \tag{13a}$$

or

$$\tau = \frac{2R}{\omega_{ac}} \quad . \tag{13b}$$

(c) Using the substitution described by (12), a corresponding n-th order digital Butterworth lowpass filter is obtained as[1]

$$G_{LP}(z) = G_{LP}(s)\Big|_{s=\frac{\omega_{ac}}{R}\frac{z-1}{z+1}}$$

$$= K\,\frac{(z+1)^n}{(z-p_1)(z-p_2)\;\ldots\;(z-p_n)}$$

$$\triangleq KG(z) \quad , \tag{14a}$$

with

$$p_i \triangleq \frac{(1+u_iR)}{(1-u_iR)} \tag{14b}$$

and, for unity gain in the low passband,

[1] Further details in the manipulation are found in Appendix C.

$$K = \frac{R^n}{(1-u_1R)(1-u_2R)\ \ldots\ (1-u_nR)}$$

$$= \frac{1}{G(1)} \quad , \tag{14c}$$

where u_i are the poles of the normalized n-th order analog Butterworth lowpass filter $G_{LPN}(s)$ described in Appendix A1.

Remark 2:

- Note that the digital filter is explicitly dependent on the factor R.
- The critical frequency will be determined by the sampling frequency through the ratio ω_{dc}/ω_s.
- The gain K may be arbitrarily chosen if so desired.

Δ

Example 1: 3rd Order Digital Butterworth Lowpass Filter

Problem: Design a 3rd order digital Butterworth lowpass filter with cut-off frequency ω_{dc}.

Solution: From Appendix A1, the normalized 3rd order analog Butterworth lowpass filter is given by

$$G_{LPN}(s) = \frac{1}{(s-u_1)(s-u_2)(s-u_3)} \quad , \tag{15a}$$

where

$$u_1 = -1 \tag{15b}$$

$$u_2 = -.5 + j.866 \tag{15c}$$

$$u_3 = -.5 - j.866 \tag{15d}$$

Following the above procedures:

(a) Select $\omega_{dc}/\omega_s = .1476$ or $\omega_s = 6.77\omega_{dc}$. With this ratio, the digital ZOH reproduction of a sine wave at ω_{dc} is approximately as shown in Fig.5 .

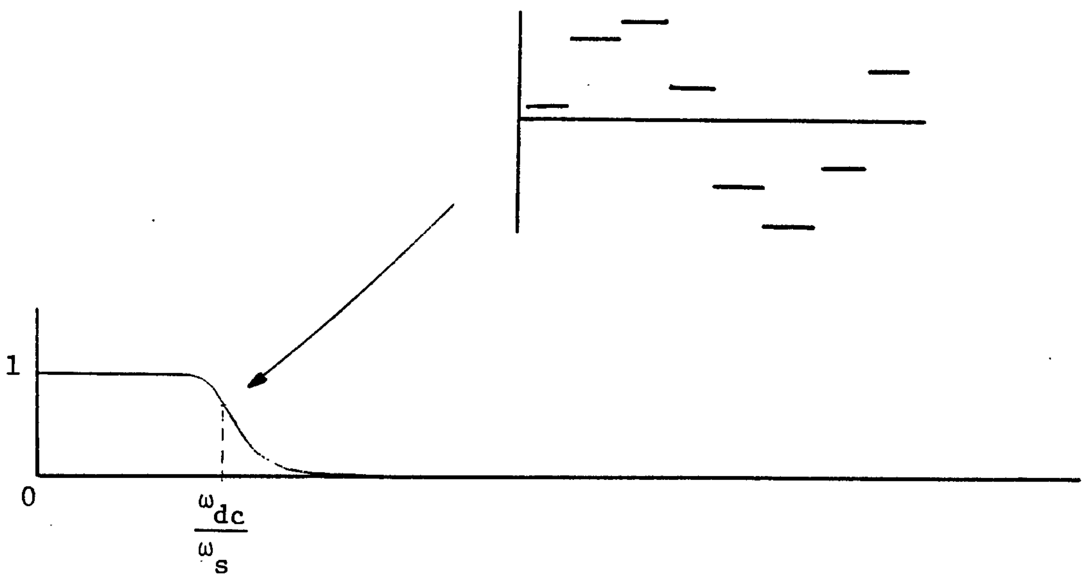

Fig.5

(b) $R = \tan(.1476\pi) = .5$ (by choice of (a)) (16)

(c) $$p_1 = \frac{1 + (-1)(.5)}{1 - (-1)(.5)} = .3333 \tag{17a}$$

$$p_2 = \frac{1 + (-.5 + j.866)(.5)}{1 - (-.5 + j.866)(.5)} = .4286 + j.4949 \tag{17b}$$

$$p_3 = \frac{1 + (-.5 - j.866)(.5)}{1 - (-.5 - j.866)(.5)} = .4286 - j.4949 = p_2^* \tag{17c}$$

$$K = \frac{(.5)^3}{(1-(-1)(.5))(1-(-.5+j.866)(.5))(1-(-.5-j.866)(.5))}$$

$$= .04762 \qquad (17d)$$

The 3rd order digital Butterworth lowpass filter is thus given by

$$G_{LP}(z) = \frac{.04762(z+1)^3}{(z-.3333)(z-.4286-j.4949)(z-.4286+j.4949)}$$

$$= \frac{.04762(z^3+3z^2+3z+1)}{z^3-1.1905z^2+.7143z-.1429} \quad . \qquad (18)$$

The theoretical frequency response of $G_{LP}(z)$ in (18), computed as $|G_{LP}(e^{j\omega T})|$ versus ω/ω_s, is shown in Fig. 6.

The recursive equation for the digital lowpass filter follows from (18) as

$$y(k) = 1.1905y(k-1) - .7143y(k-2) + .1429y(k-3)$$

$$+ .04762[u(k) + 3u(k-1) + 3u(k-2) + u(k-3)] \qquad (19)$$

where y(k) and u(k) are respectively the discrete output and input sequences of the filter. The microprocessor-based implementation of the lowpass filter given by (18) or (19) is described in Section 3. An experimental frequency response of the microprocessor-based 3rd order digital Butterworth lowpass filter is presented in Section 4.

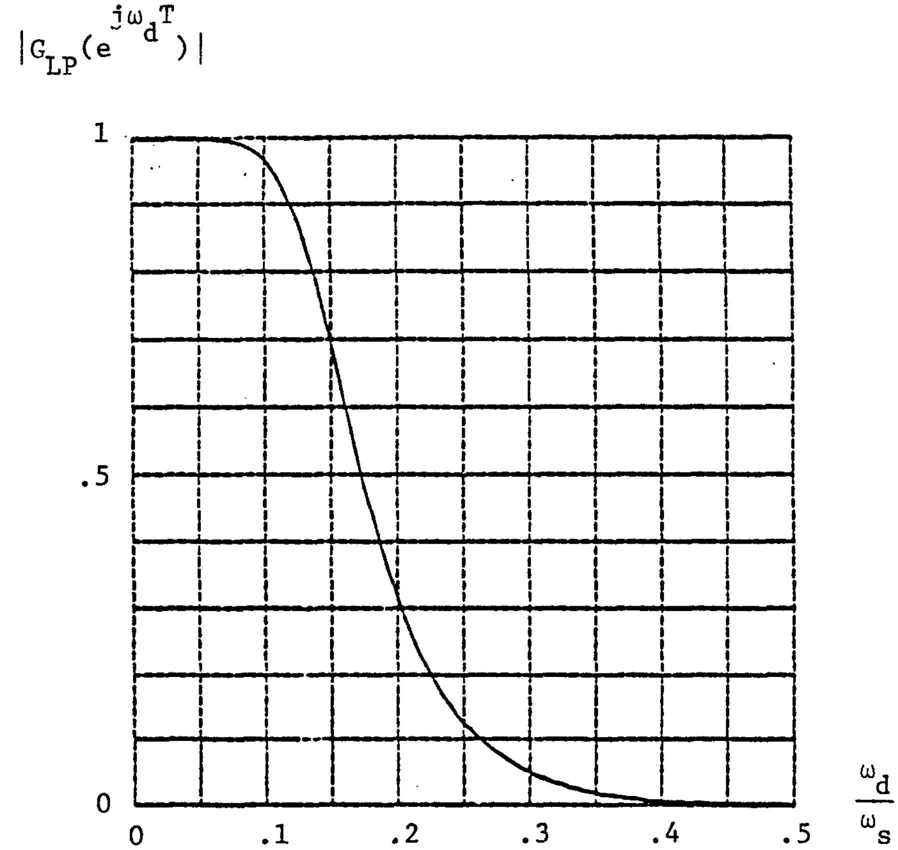

Fig. 6. Theoretical Frequency Response of $G_{LP}(z)$ in (18)

5.1.3 DESIGN OF DIGITAL HIGHPASS FILTERS

The design of an n-th order analog Butterworth highpass filter $G_{HP}(s)$ with critical cut-in frequency ω_{ac} is given in Appendix A3. The following procedure may be used to systematically obtain a corresponding digital Butterworth highpass filter $G_{HP}(z)$ from $G_{HP}(s)$.

(a) Select the desired ratio ω_{dc}/ω_s where ω_{dc} is the critical cut-in frequency of the digital highpass filter (see Fig.3b).

(b) Set

$$R = \tan\left(\frac{\omega_{dc}}{\omega_s}\pi\right)$$

$$= \frac{\omega_{ac}\tau}{2} \quad , \tag{20a}$$

so that

$$\tau = \frac{2R}{\omega_{ac}} \tag{20b}$$

(c) Using the conversion scheme (12), a corresponding n-th order digital Butterworth highpass filter is obtained as[1]

$$G_{HP}(z) = G_{HP}(s)\Big|_{s = \frac{\omega_{ac}}{R}\frac{z-1}{z+1}}$$

$$= \frac{K(z-1)^n}{(z-p_1)(z-p_2)\ \dots\ (z-p_n)}$$

$$\triangleq KG(z) \tag{21a}$$

with

---

[1] Details given in Appendix C.

$$p_i = \frac{1 + u_i R}{1 - u_i R} \tag{21b}$$

and, for unity gain in the high passband,

$$K = \frac{1}{(1 - u_1 R)(1 - u_2 R) \ \ldots \ (1 - u_n R)}$$

$$= \frac{1}{G(-1)} , \tag{21c}$$

where u_i are the poles of the normalized n-th order analog Butterworth lowpass filter $G_{LPN}(s)$ described in Appendix A1.

Remark 2 similarly applies to the above design of digital Butterworth highpass filter.

<u>Example 2</u>: 3rd Order Digital Butterworth Highpass Filter

Problem: Design a 3rd order digital Butterworth highpass filter with cut-in frequency ω_{dc}.

Solution: From Appendix A3, the 3rd order normalized analog Butterworth lowpass filter is given by

$$G_{HPN}(s) = \frac{s^3}{(s - u_1)(s - u_2)(s - u_3)} , \tag{22a}$$

where

$$u_1 = -1 \tag{22b}$$

$$u_2 = -.5 + j.866 \tag{22c}$$

$$u_3 = -.5 - j.866 \tag{22d}$$

Following the procedures outlined above:

(a) Select $\omega_{dc}/\omega_s = .05$ or $\omega_s = 20_{dc}$. With this ratio, the digital ZOH reproduction of a sine wave at ω_{dc} is approximately as shown in Fig.7.

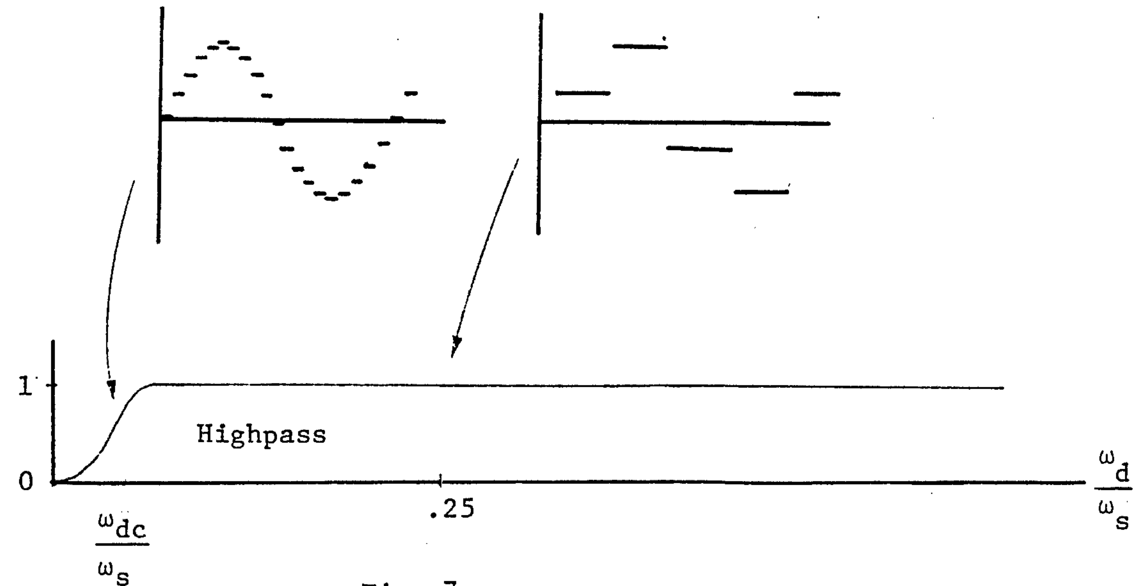

Fig. 7.

(b) $R = \tan(.05\pi) = .1585$ (23)

(c) $$p_1 = \frac{1 + (-1)(.1585)}{1 - (-1)(.1585)} = .72637 \tag{24a}$$

$$p_2 = \frac{1 + (-.5 + j.866)(.1585)}{1 - (-.5 + j.866)(.1585)} = .82366 + j.23195 \tag{24b}$$

$$p_3 = \frac{1 + (-.5 - j.866)(.1585)}{1 - (-.5 - j.866)(.1585)} = .82366 - j.23195 = p_2^* \tag{24c}$$

Hence,

$$G_{HP}(z) = \frac{K(z-1)^3}{(z-.72637)(z-.82366-j.23195)(z-.82366+j.23195)}$$

$$= \frac{K(z^3-3z^2+3z-1)}{z^3-2.3737z^2+1.9288z-.5319} \tag{25a}$$

with

$$K = 1/G(-1) = .72929 \quad . \tag{25b}$$

The theoretical frequency response of $G_{HP}(z)$ in (25), computed as $|G_{HP}(e^{j\omega T})|$ versus ω/ω_s is shown in Fig.8.

The recursive equation for the digital highpass filter follows from (25) as

$$y(k) = 2.3737y(k-1) - 1.9288y(k-2) + .5319y(k-3)$$
$$+ .72929[u(k) - 3u(k-1) + 3u(k-2) - u(k-3)] \quad , \tag{26}$$

where y(k) and u(k) are respectively the output and input sequences of the filter. The microprocessor-based implementation and experimental frequency response of the highpass filter (25) or (26) are described in Sections 3 and 4.

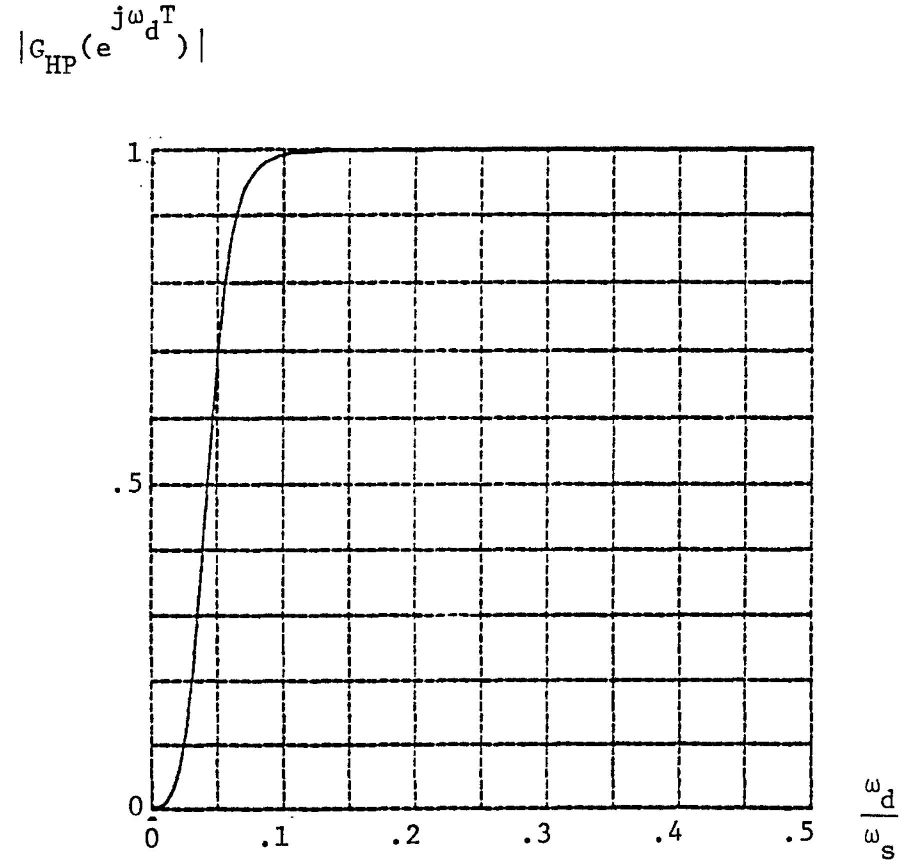

Fig. 8. Theoretical Frequency Response of $G_{HP}(z)$ given by (25).

5.1.4 DESIGN OF DIGITAL BANDPASS FILTERS

The design of a 2n-th order analog Butterworth bandpass filter $G_{BP}(s)$ with bandwidth BW and mid-band frequency ω_{ao} is given in Appendix A5. From $G_{BP}(s)$, a corresponding digital Butterworth bandpass filter $G_{BP}(z)$ can be obtained as follows:

(a) Choose ω_{do}/ω_s, where ω_{do} is the mid-band frequency of the digital filter, so that $(\omega_{do} + \frac{BW}{2})/\omega_s << .5$.

(b) Obtain

$$R = \tan\left(\frac{\omega_{do}}{\omega_s}\pi\right)$$

$$= \frac{\omega_{ao}\tau}{2} \tag{27a}$$

or

$$\tau = \frac{2R}{\omega_{ao}} \quad . \tag{27b}$$

(c) Invoking the conversion scheme, a corresponding 2n-th order digital Butterworth bandpass filter can be obtained as[1,2]

$$G_{BP}(z) = G_{BP}(s)\Big|_{s = \frac{2}{\tau}\frac{z-1}{z+1}}$$

$$= \frac{K(z-1)^n(z+1)^n}{(z-p_1)(z-p_1^*)\ \ldots\ (z-p_n)(z-p_n^*)} \tag{28a}$$

---

1 * denotes complex conjugation.

2 Details of manipulation is given in Appendix C.

with

$$p_i \triangleq \frac{(2/\tau + c_i)}{(2/\tau - c_i)} \quad , \qquad i = 1, \ldots, n, \tag{28b}$$

$$c_i \triangleq \frac{BW}{2} u_i \pm j\omega_{ao} \quad , \tag{28c}$$

$$K \triangleq \frac{(BW)^n (2/\tau)^n}{\prod_{i=1}^{n} (2/\tau - c_i)(2/\tau - c_i^*)} \quad , \tag{28d}$$

where τ is given by (27).

Remark 3: The design of the bandpass filter (28) assumes that $|BWu_i|^2 << 4\omega_{ao}^2$ (see Appendix A5). This is equivalent to considering a bandpass filter with a high Q-factor (the ratio of the midband frequency to the bandwidth), i.e.,

$$Q \triangleq \frac{\omega_{ao}}{BW} \geq 1. \tag{29}$$

Δ

Example 3: 6th Order Digital Butterworth Bandpass Filter

Problem: Design a 6th order digital Butterworth bandpass filter with bandwidth of $BW = 2\pi \times 20$ rad/s and midband frequency of $\omega_{do} = 2\pi \times 20$ rad/s. (Note the Q-factor = $\frac{\omega_o}{BW} = 1.$)

Solution: From Appendix A5, a 6th order analog Butterworth bandpass filter having the above specification ($BW = 2\pi \times 20$, $\omega_{ao} = \omega_{do} = 2\pi \times 20$) is given by

$$G_{BP}(s) = \frac{(BW)^3 s^3}{(s - c_1)(s - c_1^*)(s - c_2)(s - c_2^*)(s - c_3)(s - c_3^*)} \quad (30a)$$

with

$$c_1, c_1^* = \frac{(2\pi \times 20)(-1)}{2} \pm j2\pi \times 20$$

$$= -20\pi \pm j40\pi \quad (30b)$$

$$c_2, c_3 = \frac{(2\pi \times 20)}{2}(-.5 + j.866) \pm j2\pi \times 20$$

$$\doteq -10\pi + j57.32\pi, \qquad -10\pi - j22.68\pi \quad (30c)$$

$$c_2^*, c_3^* = -10\pi - j57.32\pi, \qquad -10\pi + j22.68\pi \quad . \quad (30d)$$

(a) Select $\omega_{do}/\omega_s = .2$ or $\omega_s = 5\omega_{do}$. With this ratio, the relative position of the passband with respect to the sampling frequency is approximately as shown in Fig. 9.

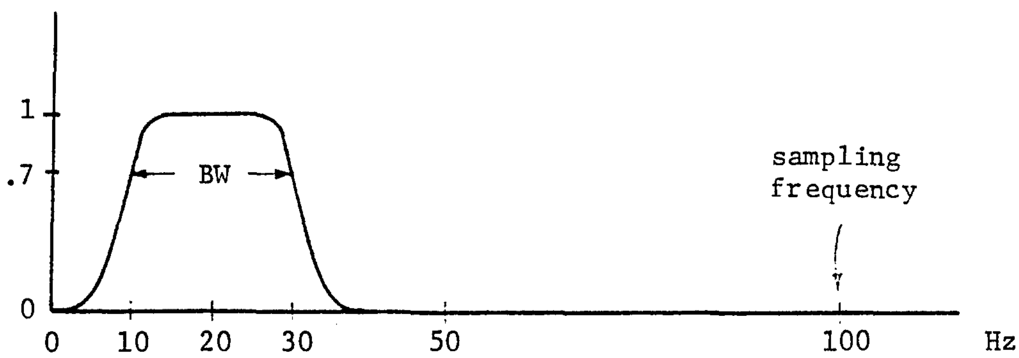

Fig. 9. BandPass Filter

(b) $R = \tan(.2\pi) \approx .73$

$$\frac{2}{\tau} = 172 \tag{31}$$

(c) $$p_1, p_1^* = \frac{172 + (-20\pi \pm j40\pi)}{172 - (-20\pi \pm j40\pi)} = .6246e^{\pm j1.3476}$$

$$= .1382 \pm j.6091 \approx .14 \pm j.61 \tag{32a}$$

$$p_2, p_2^* = \frac{172 + (-10\pi \pm j57.32\pi)}{172 - (-10\pi \pm j57.32\pi)} = .8409e^{\pm j1.6326}$$

$$= -.0519 \pm j.8393 \approx -.052 \pm j.84 \tag{32b}$$

$$p_3, p_3^* = \frac{172 + (-10\pi \pm j22.68\pi)}{172 - (-10\pi \pm j22.68\pi)} = .7319e^{\pm j.8194}$$

$$= .4996 \pm j.5348 \simeq .50 \pm j.53 \tag{32c}$$

$$(\frac{2}{\tau} - c_1)(\frac{2}{\tau} - c_1^*) = 266.35^2$$

$$(\frac{2}{\tau} - c_2)(\frac{2}{\tau} - c_2^*) = 271.68^2$$

$$(\frac{2}{\tau} - c_3)(\frac{2}{\tau} - c_3^*) = 215.54^2$$

$$K = \frac{(2\pi \times 20)^3 (172)^3}{266.35^2 \times 271.68^2 \times 215.54^2} = .0415 \tag{32d}$$

Hence,

$$G_{BP}(z) \simeq \frac{0.0415(z - 1)^3 (z + 1)^3}{(z - .14 - j.61)(z - .14 + j.61)(z + .052 - j.84)(z + .052 + j.84)}$$

$$\times \frac{1}{(z - .5 - j.53)(z - .5 + j.53)}$$

$$= \frac{0.0415(z^6 - 3z^4 + 3z^2 - 1)}{(z^6 - 1.176z^5 + 1.7778z^4 - 1.3219z^3 + 1.0035z^2 - .3611z + .1473)} \tag{33}$$

The theoretical frequency response of $G_{BP}(z)$ in (33), computed as $|G_{BP}(e^{j\omega T})|$ versus ω/ω_s, is shown in Fig. 10.

The recursive equation for the 6th order digital bandpass filter follows from (33) as

$$y(k) = 1.176y(k-1) - 1.7778y(k-2) + 1.3219y(k-3) - 1.0035y(k-4)$$

$$+ .3611y(k-5) - .1473y(k-6) + .0415u(k) - .1245u(k-2) + .1245u(k-4)$$

$$- .0415u(k-6) \tag{34}$$

where y(k) and u(k) are respectively the output and input of the filter. The microprocessor-based implementation and the experimental frequency response of the bandpass filter (33) or (34) are given in Sections 3 and 4.

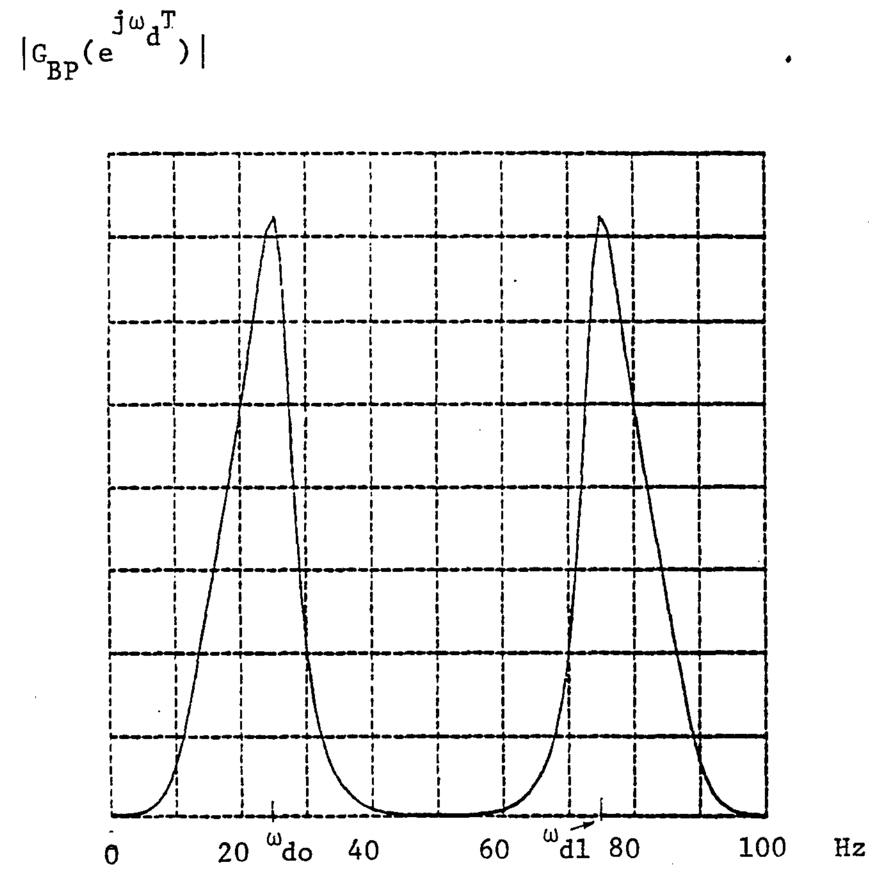

Fig. 10. Theoretical Frequency Response of $G_{BP}(z)$ given by (33).

5.1.5 DESIGN OF DIGITAL BANDSTOP FILTERS

The design of a 2n-th order Butterworth bandstop filter $G_{BS}(s)$ with bandwidth BW and midband frequency ω_{ao} is given in Appendix A6. Using $G_{BS}(s)$, a corresponding digital Butterworth bandstop filter $G_{BP}(z)$ can be obtained as follows:

(a) Choose ω_{do}/ω_s, where ω_{do} is the desired midband frequency of the digital filter, so that $(\omega_{do} + \frac{BW}{2})/\omega_s << .5$.

(b) Obtain

$$R = \tan\left(\frac{\omega_{do}}{\omega_S}\pi\right) = \frac{\omega_{ao}\tau}{2} \quad , \tag{35a}$$

so that

$$\tau = \frac{2R}{\omega_{ao}} \quad . \tag{35b}$$

(c) Using the bilinear transformation, a corresponding 2n-th order digital Butterworth bandstop filter can be obtained as

$$G_{BS}(z) = G_{BS}(s)\Big|_{s = \frac{2}{\tau}\frac{z-1}{z+1}}$$

$$= \frac{K(z - z_o)^n(z - z_o^{-1})^n}{(z - p_1)(z - p_1^*) \ldots (z - p_n)(z - p_n^*)} \quad , \tag{36a}$$

where

$$p_i \triangleq \frac{2/\tau + c_i}{2/\tau - c_i} \quad , \tag{36b}$$

$$c_i \triangleq \frac{BW}{2} u_i \pm j\omega_{ao} \quad , \quad \text{(see Appendix A5)} \tag{36c}$$

$$K \triangleq \frac{[(2/\tau)^2 + \omega_{ao}^2]^n}{(2/\tau - c_1)(2/\tau - c_1^*) \ldots (2/\tau - c_n)(2/\tau - c_n^*)} , \quad (36e)$$

$$z_\sigma = (2/\tau - j\omega_{ao})/(2/\tau + j\omega_{ao}) . \quad (36f)$$

Example 4: 6th Order Digital Butterworth Bandstop Filter

Problem: Design a 6th order digital Butterworth bandstop filter with $BW = 2\pi \times 20$ rad/s and midband frequency of $\omega_{do} = 2\pi \times 20$ rad/s. (Note the Q-factor = $\omega_{do}/BW = 1$.)

Solution: From Appendix A6, a 6th order analog Butterworth bandstop filter having the above specification ($BW = 2\pi \times 20$ and $\omega_{ao} = \omega_{do} = 2\pi \times 20$) is given by

$$G_{BS}(s) = \frac{(s^2 + \omega_{ao}^2)^3}{(s - c_1)(s - c_1^*)(s - c_2)(s - c_2^*)(s - c_3)(s - c_3^*)} \quad (37a)$$

$$c_1, c_1^* = -20\pi \pm j40\pi \quad (37b)$$

$$c_2, c_2^* = -10\pi \pm j57.32\pi \quad (37c)$$

$$c_3, c_3^* = -10\pi \pm j22.68\pi \quad . \quad (37d)$$

We note that c_i in (37) are the same as those of (30) due to certain similarities in the design specification of Examples 3 and 4. For convenience, let us also choose the design variables as in Example 3. That is:

(a) $\omega_{do}/\omega_s = .2$. With this ratio, the relative position of the stopband with respect to the sampling frequency is approximately as shown in Fig. 11 ,

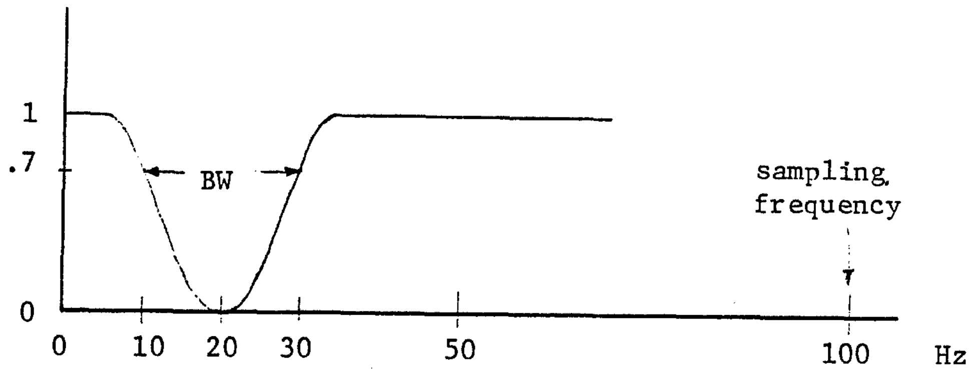

Fig. 11. Bandstop Filter

(b) $R = \tan(.2\pi) \simeq .73$,

$2/\tau = 172$; (38)

(c) $p_1, p_1^* = .14 \pm j.61,$

$p_2, p_2^* = -.052 \pm j.84$, (39)

$p_3, p_3^* = .50 \pm j.53$,

$$(\frac{2}{\tau} - c_1)(\frac{2}{\tau} - c_1^*) = 266.35^2 \quad ,$$

$$(\frac{2}{\tau} - c_2)(\frac{2}{\tau} - c_2^*) = 271.68^2 \quad , \tag{40}$$

$$(\frac{2}{\tau} - c_3)(\frac{2}{\tau} - c_3^*) = 215.54^2 \quad .$$

In addition, we compute

$$(\frac{2}{\tau})^2 + \omega_{ao}^2 = 172^2 + (2\pi \times 20)^2 = 45375 \tag{41a}$$

so that (36e) yields

$$K = \frac{45375^3}{266.35^2 \times 271.68^2 \times 215.54^2} = .384 \quad . \tag{41b}$$

The zeroes specified by (36d) are given by

$$z_o = \frac{172 + j2\pi \times 20}{172 - j2\pi \times 20} = e^{-j1.2619} = .3040 - j.9527 \tag{42a}$$

$$z_o^{-1} = .3040 + j.9527 \quad . \tag{42b}$$

From the above, the corresponding 6th order digital Butterworth bandstop filter is obtained as

$$G_{BS}(z) = \frac{.384(z - .3040 + j.9527)^3(z - .3040 - j.9527)^3}{(z - .14 - j.61)(z - .14 + j.61)(z + .052 - j.84)(z + .052 + j.84)}$$

$$\times \frac{1}{(z - .5 - j.53)(z - .5 + j.53)}$$

$$= \frac{.384(z^6 - 1.824z^5 + 4.109z^4 - 3.873z^3 + 4.109z^2 - 1.824z + 1)}{z^6 - 1.176z^5 + 1.7778z^4 - 1.3219z^3 + 1.0035z^2 - .3611z + .1473} \quad (43)$$

The theoretical frequency response of $G_{BS}(z)$ in (43), computed as $|G_{BS}(e^{j\omega T})|$ versus ω/ω_s is shown in Fig.12.

The recursive equation for the 6th order Butterworth bandstop filter follows from (43) as

$$\begin{aligned} y(k) = {} & 1.176y(k-1) - 1.7778y(k-2) + 1.3219y(k-3) - 1.0035y(k-4) \\ & + .3611y(k-5) - .1473y(k-6) + .384[u(k) - 1.824u(k-1) + 4.109u(k-2) \\ & - 3.873u(k-3) + 4.109u(k-4) - 1.824u(k-5) + u(k-6)], \end{aligned} \quad (44)$$

where y(k) and u(k) are respectively the output and input of the digital filter. The microprocessor-based implementation and the experimental frequency response of the bandstop filter (43) or (44) are given in Sections 3 and 4.

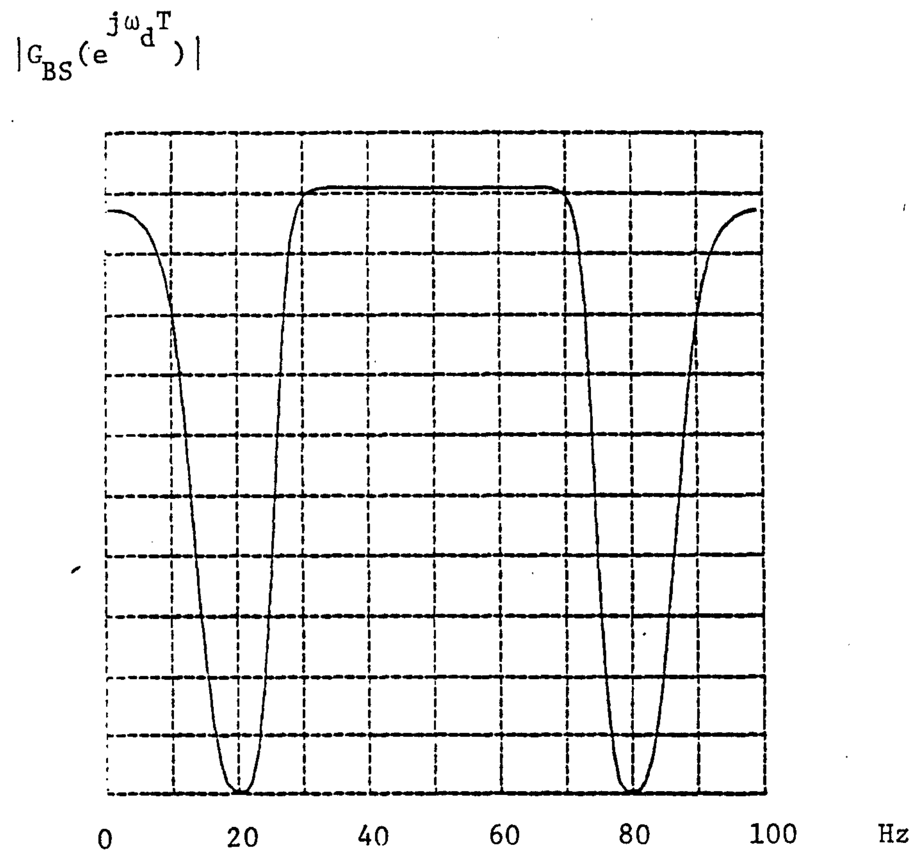

Fig. 12. Theoretical Frequency Response of $G_{BS}(z)$ given by (43).

5.1.6 A FURTHER EXAMPLE

The effect of pole variation in the filter may be vividly illustrated by considering the following example.

Example 5: 3rd Order Digital Chebychev Lowpass Filter

Problem: Design a 3rd order digital Chebychev lowpass filter with cut-off frequency ω_{dc}, having a ripple factor r = 1 db. Similar design considerations for Example 1 may be used.

Solution: Let a 3rd order analog Chebychev lowpass filter be denoted by

$$G_{LPC}(s) = \frac{K_a}{(s - u_1')(s - u_2')(s - u_3')} \tag{45}$$

where the poles u_1', u_2' and u_3' may be determined as follows.

The specification of the filter translates into the frequency response sketched in Fig. 13. The ripple factor

$$\begin{aligned} r &= 1 \\ &= 20 \log(1) - 20 \log\left(\frac{1}{\sqrt{1 + \varepsilon^2}}\right) \\ &= 10 \log(1 + \varepsilon^2), \end{aligned} \tag{46a}$$

so that

$$\begin{aligned} \varepsilon &= \sqrt{10^{r/10} - 1} \\ &= .5088 \quad ,(r = 1) \quad . \end{aligned} \tag{46b}$$

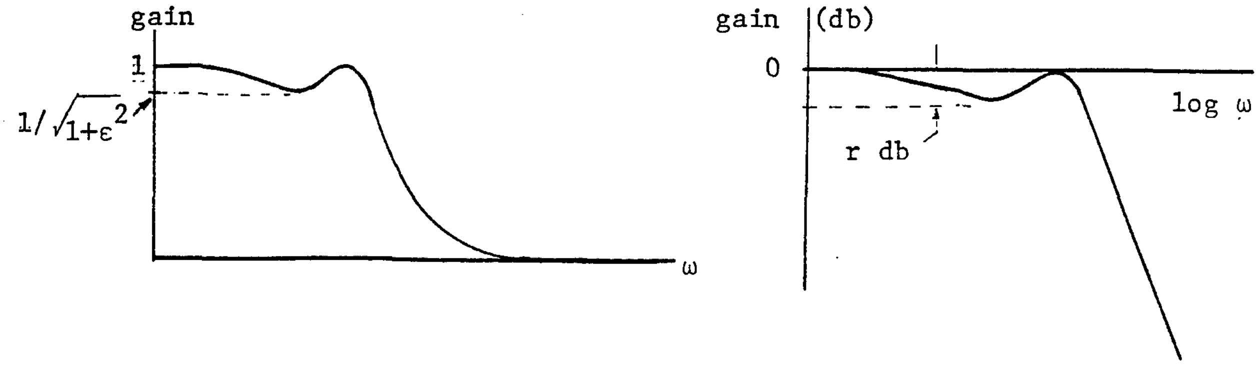

Fig. 13. Chebychev Lowpass Filter

Let n = 3 denote the order of the filter and define

$$a = \frac{1}{n} \sinh\left(\frac{1}{\varepsilon}\right)$$

$$= \frac{1}{n} \ln\left(\frac{1}{\varepsilon} + \sqrt{\left(\frac{1}{\varepsilon}\right)^2 + 1}\right)$$

$$= \frac{1}{3} \ln\left(\frac{1}{.5088} + \sqrt{\left(\frac{1}{.5088}\right)^2 + 1}\right)$$

$$= .4760 \,, \tag{47a}$$

so that

$$\tanh a = \frac{e^{a} - e^{-a}}{e^{a} + e^{-a}}$$

$$= .4430 \,. \tag{47b}$$

The poles of the analog Chebychev lowpass filter may be treated as being the poles of the analog Butterworth lowpass filter whose real parts are reduced by a factor of tanh a. Using the values of u_i in Example 1, the poles of the "normalized" analog Cheybechev filter (45) can hence be determined from

$$u_i' = \text{Re}\,\{u_i\} \times \tanh a + j\text{Im}\{u_i\}. \tag{48}$$

as

$$u_1' = -.443 \tag{49a}$$

$$u_2' = -.2215 + j.866 \tag{49b}$$

$$u_3' = -.2215 - j.866 \quad . \tag{49c}$$

Using relationship (14b), the poles u_i' in the s-domain can be mapped into the poles in the z-domain as

$$p_i' = \frac{(1 + u_i'R)}{(1 - u_i'R)} \quad . \tag{50}$$

With the same choice of R as in Example 1 (i.e., R = .5), we obtain

$$p_1' = \frac{1 + (-.443)(.5)}{1 - (-.443)(.5)} = .644 \tag{51a}$$

$$p_2' = \frac{1 + (-.2215 + j.866)(.5)}{1 - (-.2215 + j.866)(.5)} = .8269e^{j.8247} = .563 + j.609 \tag{51b}$$

$$p_3' = p_2'^{*} = .563 - j.609 \quad . \tag{51c}$$

Hence, a corresponding 3rd order digital Chebychev lowpass filter can be obtained as

$$G_{LPC}(z) = \frac{K(z + 1)^3}{(z - p_1')(z - p_2')(z - p_3')} \tag{52}$$

$$= \frac{K(z+1)^3}{(z-.644)(z-.563-j.609)(z-.563+j.609)}$$

$$= \frac{K(z^3+3z^2+3z+1)}{(z^3-1.77z^2+1.413z-.443)}$$

$$\triangleq KG(z) \quad , \tag{52a}$$

where for unity gain at the low frequency

$$K = \frac{1}{G(1)} = \frac{.2}{8} = .025 \quad . \tag{52b}$$

The theoretical frequency response of $G_{LPC}(z)$ given by (52), computed as $|G_{LPC}(e^{j\omega T})|$ versus ω/ω_s is shown in Fig. 14.

The recursive equation for the 3rd order Chebychev lowpass filter follows from (52) as

$$\begin{aligned} y(k) = {} & 1.77y(k-1) - 1.413y(k-2) + .443y(k-3) \\ & + .025u(k) + .075u(k-1) + .075u(k-2) + .025u(k-3) \ , \end{aligned} \tag{53}$$

where y(k) and u(k) are the output and the input of the digital filter. The microprocessor-based implementation and experimental frequency response of the digital Chebychev lowpass filter (52) or (53) are given in Sections 3 and 4.

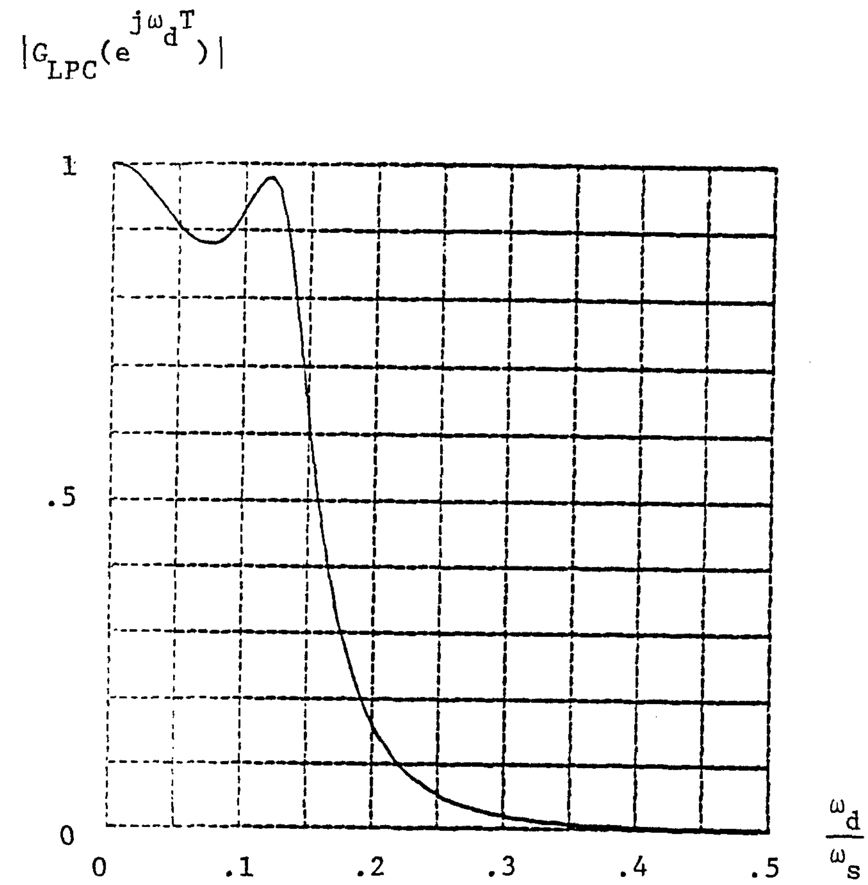

Fig. 14. Theoretical Frequency Response of $G_{LPC}(z)$ given by (52).

5.2 MICROPROCESSOR REALIZATION OF DIGITAL FILTERS

The microprocessor firmware for implementing the digital frequency selective filters designed in Section 2 is described below.

Fig.15 shows the block diagrams of the hardware for the microprocessor-based signal processing system used in the realization of the digital filters. The CPU of the system is the Motorola MC6802 microprocessor, which is supported by 2716 EPROM (monitor program), 6810 RAM's, 6821 PIA's, keypad, L.E.D. display and interfacing buffers to form the microcomputer called MOUSE[1] (see Fig.16). The microcomputer operates at a clock rate of 1 MHz.

The data acquisition unit is the Datel MDAS-16 multiple (multiplex) channel 12-bit A/D converter with a conversion time of about 20 μs per data. A Datel Hz12BGC 12 bit D/A converter with a settling time of 3 μs is used as a zero-order-hold output of the microprocessor-based system. The interface between the 8-bit MC6802 and the 12-bit I/O (A/D and D/A) peripherals are done through 6821 PIA's (Fig.17). The software (< 1k bytes) for the digital filters are stored in the external 2716 EPROM. The additional 2114 RAM's provide handy facilities for debugging and immediate alterations of the software if desired. The wiring diagrams for the microprocessor-based signal processing system is shown in Figs. 16 and 17.

[1] Acronymn for Microcomputer of Oakland University School of Engineering.

The main consideration in the microprocessor software for the digital filters involves the development of fast and efficient arithmetic subroutines, the scaling of the recursive digital filter equations, the handling of saturation and some memory management.

A fast 3 bytes x 1 byte multiplication subroutine with an execution time of about 96 μs was developed for the digital filter implementation. Other main subroutines include a 3 bytes + 3 bytes summation (about 85 μs), transfer and negation of 3 byte data. Details of these subroutines are given in Appendix B.

In order to minimize the occurrence of saturation (overflow or underflow) in the finite wordlength data (3 bytes or 24 bits), the recursive formulas for each of the filters will be scaled in a fashion similar to those done in an analog computer simulation. The scaled recursive equations for the digital filters from Examples 1 - 5, are shown in Table 1.

It is remarked that the forward gains K of the filters may be reduced, if necessary, to achieve a proper scaling which will not saturate the filter output. Alternatively, the output saturation can be handled by use of overflow test instructions in the microprocessor software.

The 6802 microprocessor software for implementing the digital frequency selective filters described in Table 1 are given in Appendix B.

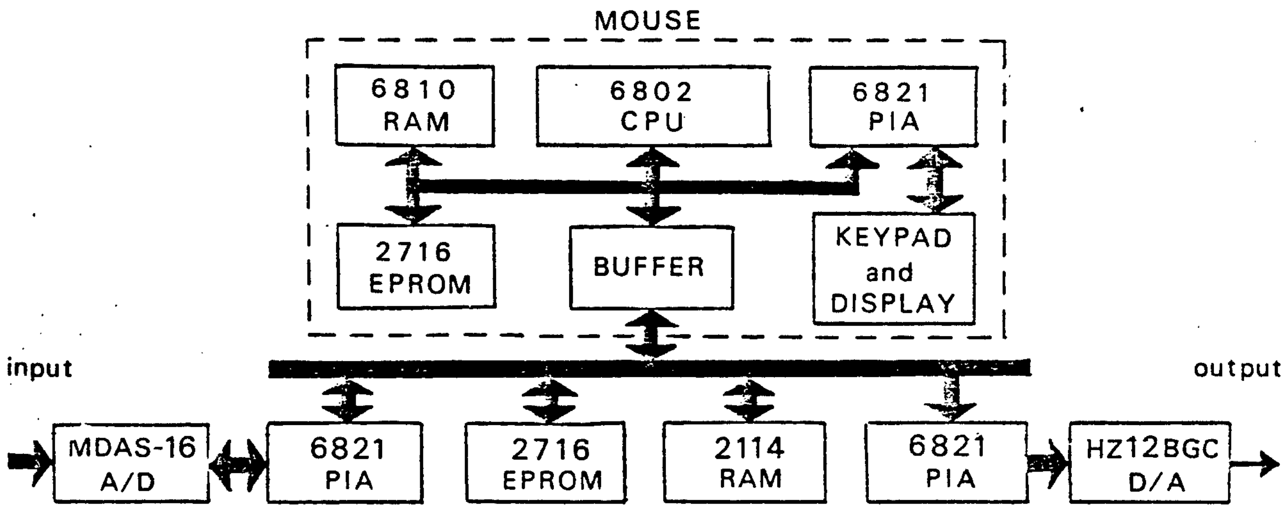

Fig. 15 Block Diagram of Microprocessor System

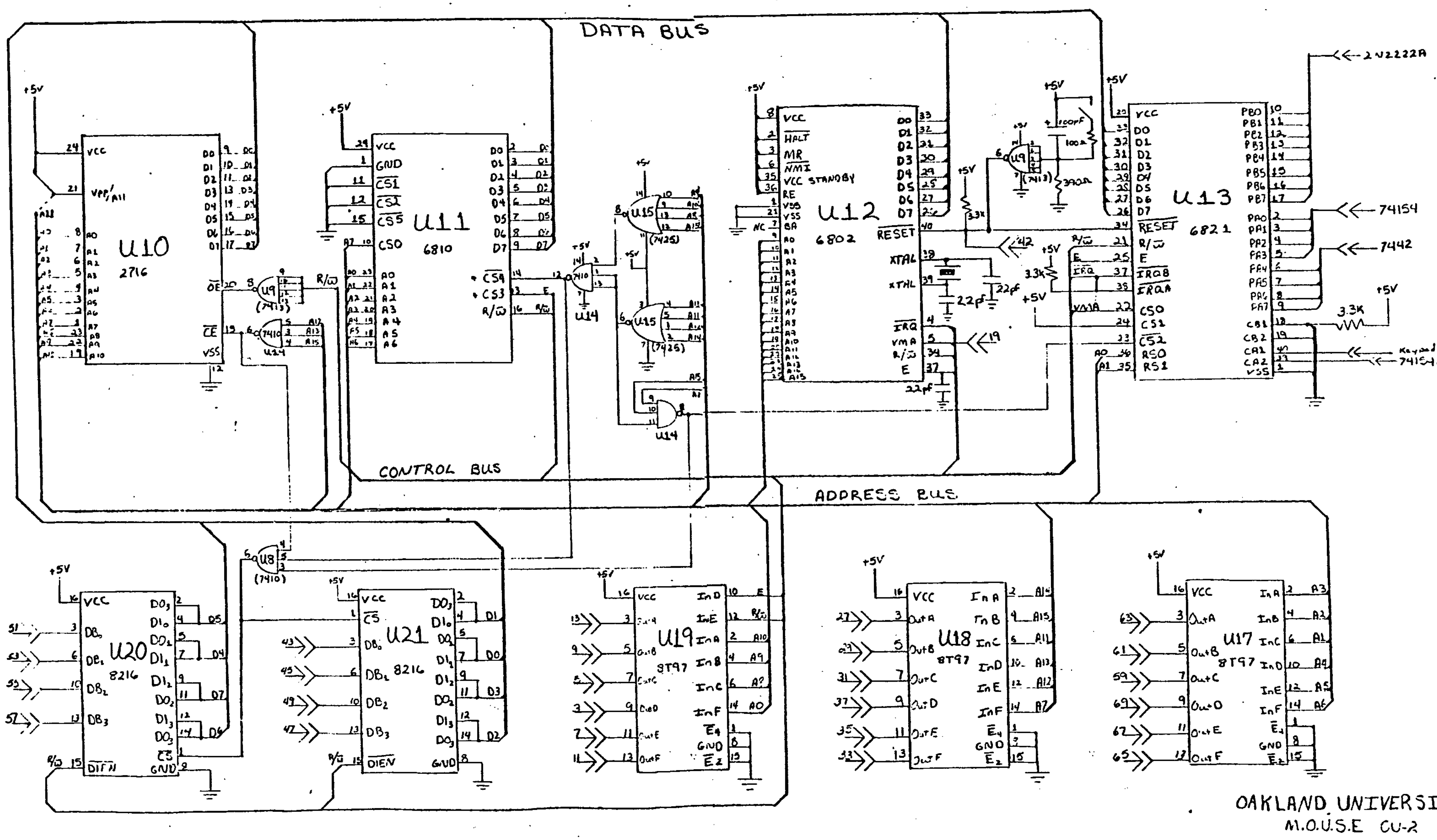

Fig. 16a Schematic for MOUSE (reference[9])

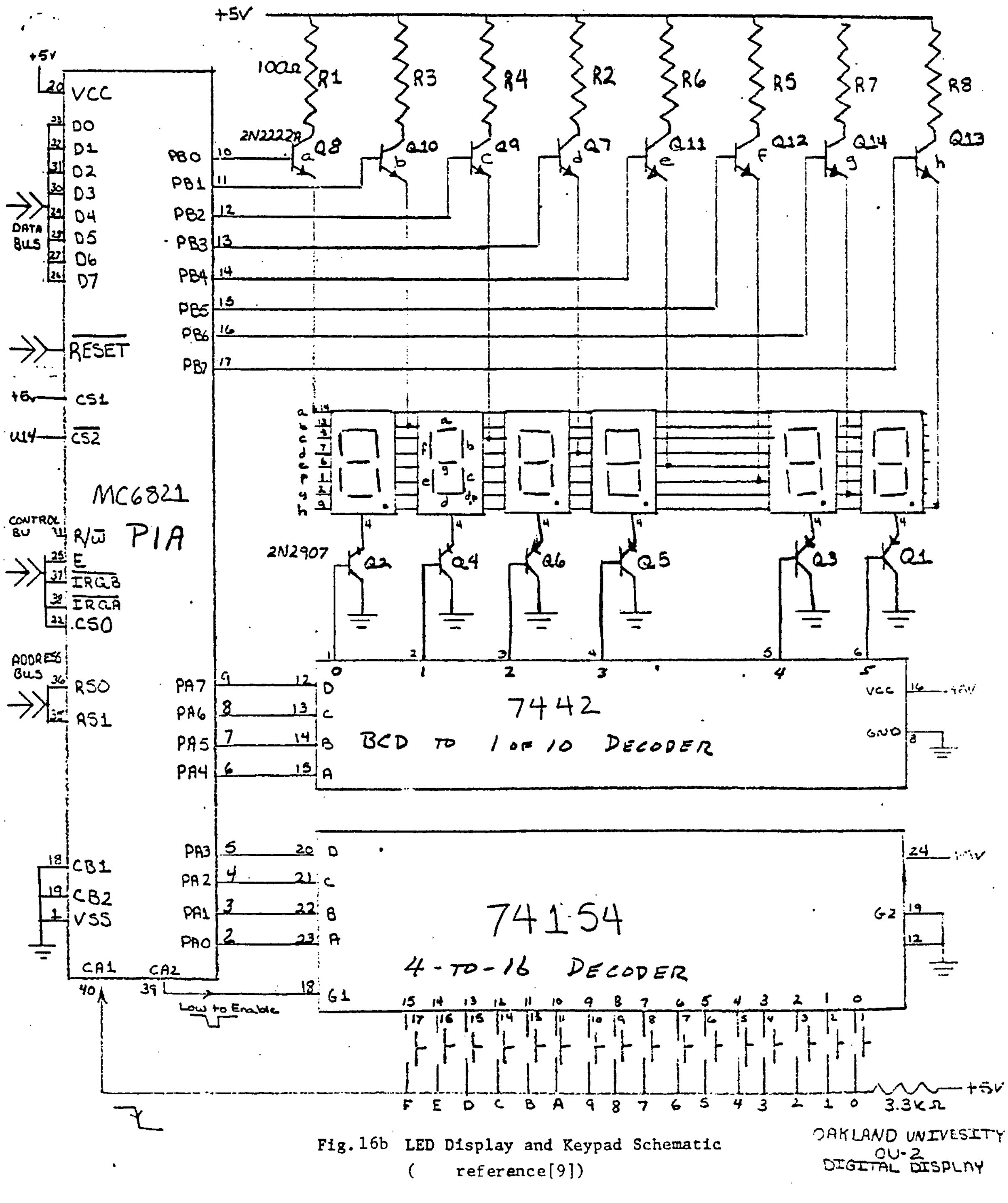

Fig. 16b LED Display and Keypad Schematic
(reference[9])

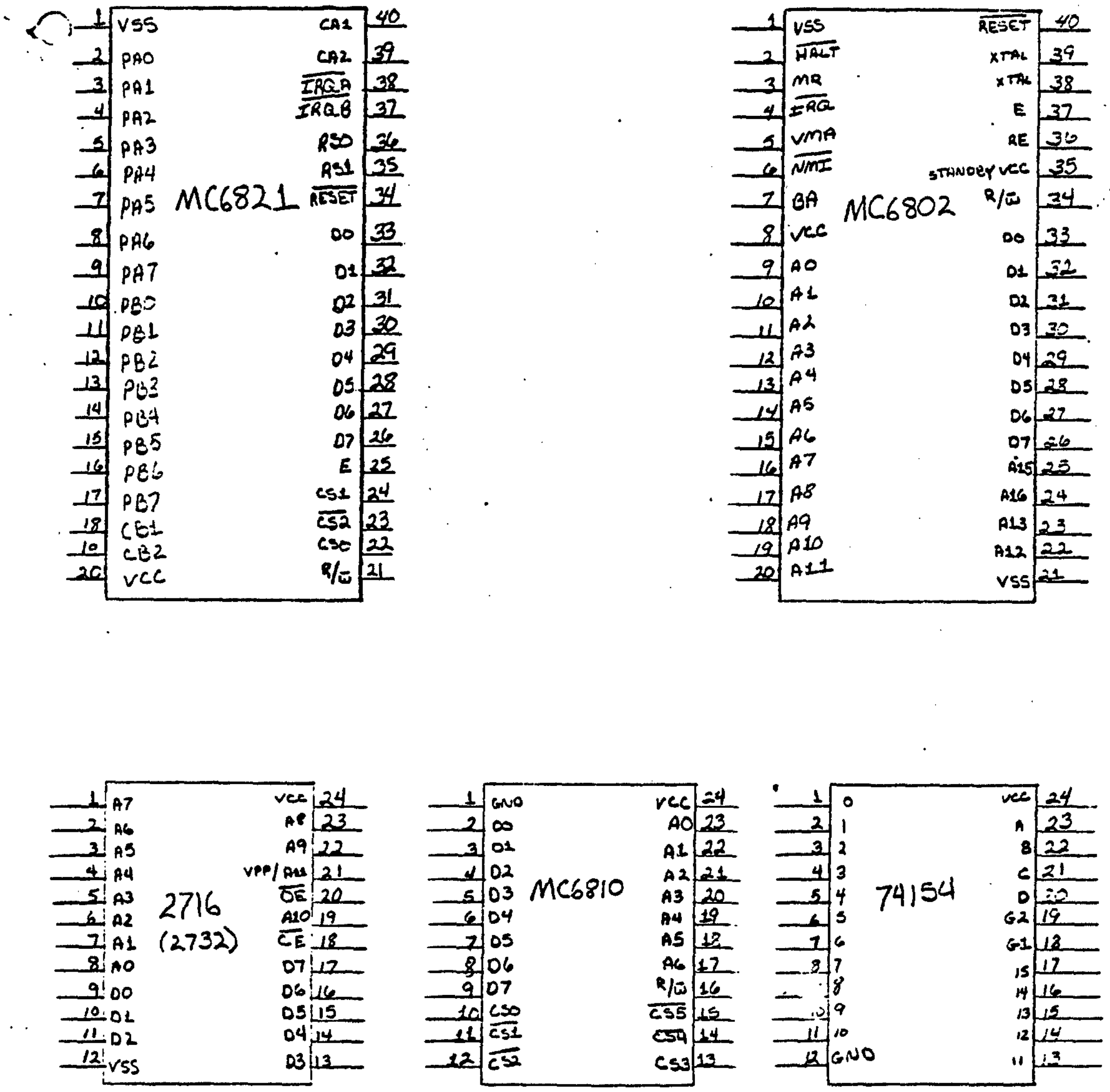

Fig. 16c Pinouts of major chips on MOUSE
(reference [9])

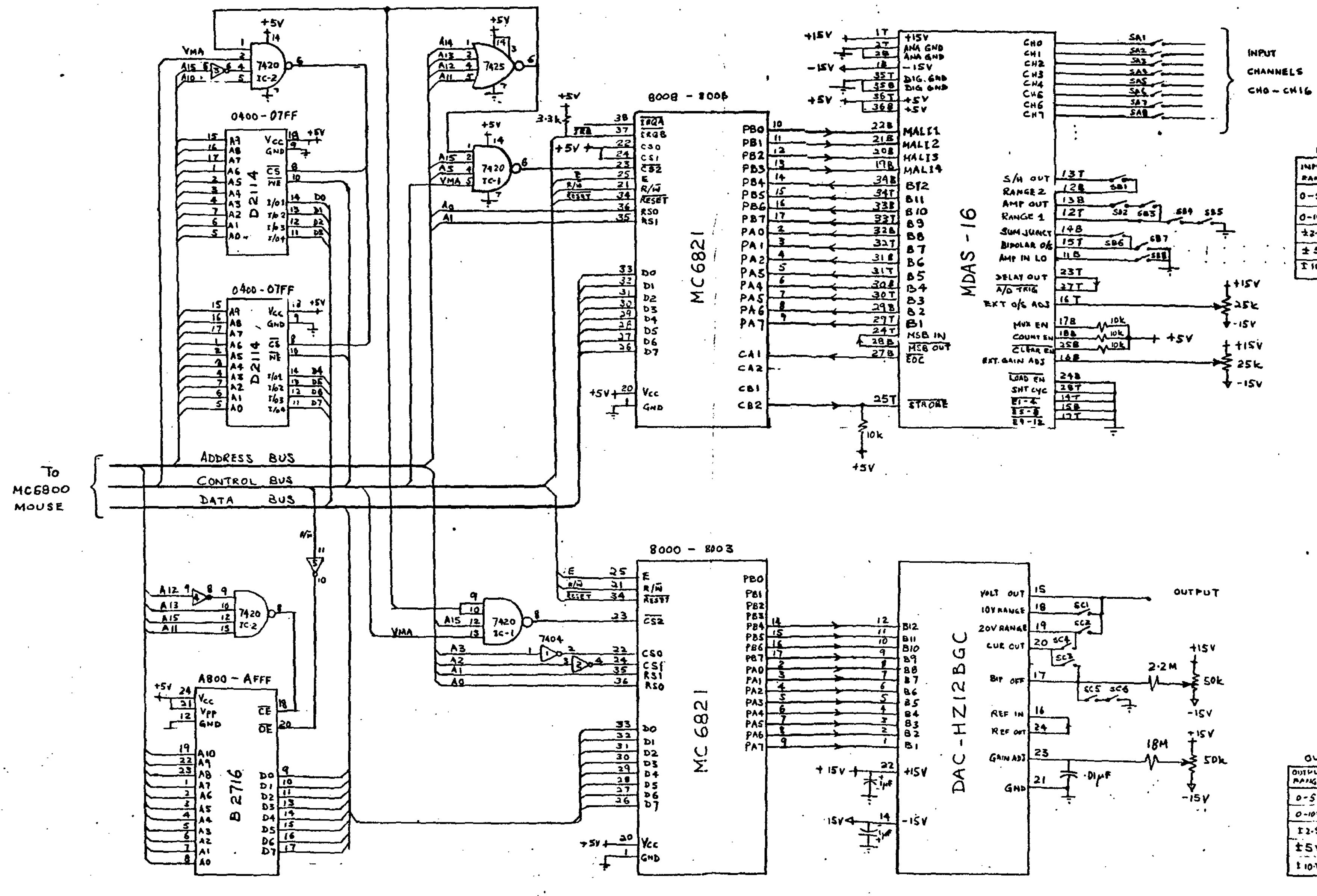

INPUT RANGE SELECTION

INPUT RANGE	SB1	SB2	SB3	SB4	SB5	SB6	SB7	SB8
0-5V	C	C	C	O	O	O	C	C
0-10V	C	O	O	C	C	O	C	C
±2.5V	C	C	C	O	O	C	O	C
±5V	C	O	O	C	C	C	O	C
±10V	O	O	O	C	C	C	O	C

OUTPUT RANGE SELECTION

OUTPUT RANGE	SC1	SC2	SC3	SC4	SC5	SC6	SC7	SC8
0-5V	C	O	O	C	C	C		
0-10V	C	O	O	O	C	C		
±2.5V	C	O	C	C	O	O		
±5V	C	O	C	O	O	O		
±10V	O	C	C	O	O	O		

Fig.17 MICROPROCESSOR CONTROLLED ADC & DAC

Table 1: SCALED RECURSIVE EQUATIONS FOR THE DIGITAL FILTERS

Butterworth Low-Pass (Example 1)

$$.84y(k) = y(k-1) - .6y(k-2) + .12y(k-3) + .04u(k) + .12u(k-1) + .12u(k-2) + .04u(k-3)$$

Butterworth High-Pass (Example 2)

$$.4213y(k) = y(k-1) - .8126y(k-2) + .2241y(k-3) + .3072u(k) - .9217u(k-1) + .9217u(k-2) - .3072u(k-3)$$

Butterworth Band-Pass (Example 3)

$$.5625y(k) = .6615y(k-1) - y(k-2) + .7436y(k-3) - .5645y(k-4) + .2031y(k-5) - .0829y(k-6) + .0233u(k) - .0700u(k-2) + .0700u(k-4) - .0233u(k-6)$$

Butterworth Band-Stop (Example 4)

$$.5625y(k) = .6615y(k-1) - y(k-2) + .7436y(k-3) - .5645y(k-4) + .2031y(k-5) - .0829y(k-6) + .216u(k) - .394u(k-1) + .8875u(k-2) - .8366u(k-3) + .8875u(k-4) - .394u(k-5) + .216u(k-6)$$

Chebychev Low-Pass (Example 5)

$$.565y(k) = y(k-1) - .7983y(k-2) + .2503y(k-3) + .0141u(k) + .0423u(k-1) + .0423u(k-2) + .0141u(k-3)$$

5.3 EXPERIMENTAL FREQUENCY RESPONSE OF MICROPROCESSOR-BASED DIGITAL FILTERS

The experimental set-up for recording the frequency response of the microprocessor-based digital filters is shown in Fig. 18 . The test input u(t), generated by the voltage controlled oscillator, consists of a constant amplitude sinusoidal signal whose frequency modulates or sweeps (sufficiently) slowly from low frequency to high frequency and vice versa, i.e.,

$$u(t) = A \sin \omega t$$

where the frequency ω is controlled by a triangular or saw-tooth signal w(t). The digital output of the filter is recorded on a storage scope whose horizontal axis is driven by the same w(t). From the set-up, one can experimentally determine the frequency responses of the microprocessor-based digital filters. Figs. 19-23 show the actual experimental frequency responses of the microprocessor-based 3rd order filters designed in the examples of Section 2.

For comparison, the critical frequencies of the theoretical filters and the implemented microprocessor-based filters are tabulated in Table 2. As shown in the table, the specification of the filters in terms of ω_{dc}, ω_{do} and BW have been met satisfactorily.

It is important to note that the critical frequencies ω_{dc} and ω_{do} can readily be altered by simply adjusting the sampling frequency ω_s. There is, however, an upper bound on the maximum possible sampling frequency which can be used for the filter due to the finite speed of the microprocessor. Nevertheless, the design specifications concerned in the present investigation can be satisfactorily fulfilled by the current generation of 8-bit microprocessors. For more stringent design specifications, one may resort to the new generation of 16-bit microprocessors and/or use of high speed arithmetic logic chips.

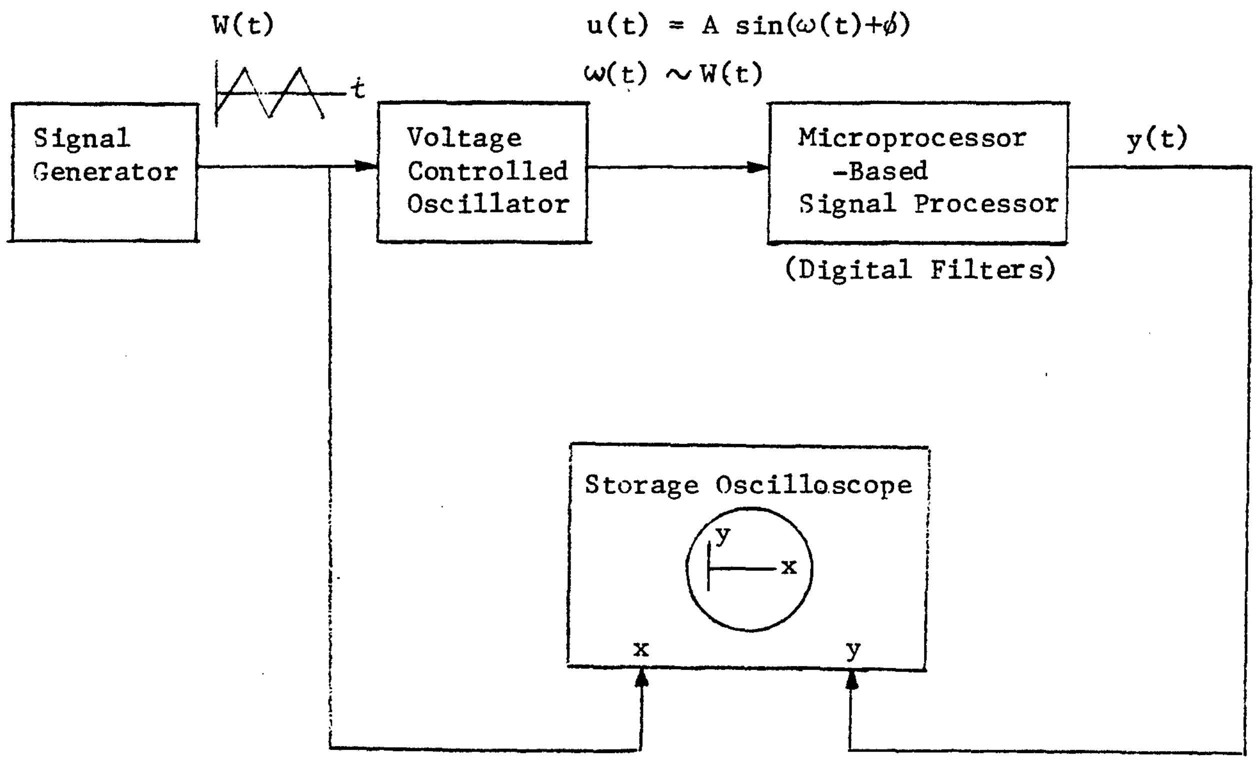

Fig. 18 Experimental Set-up for Measurement of Frequency Response

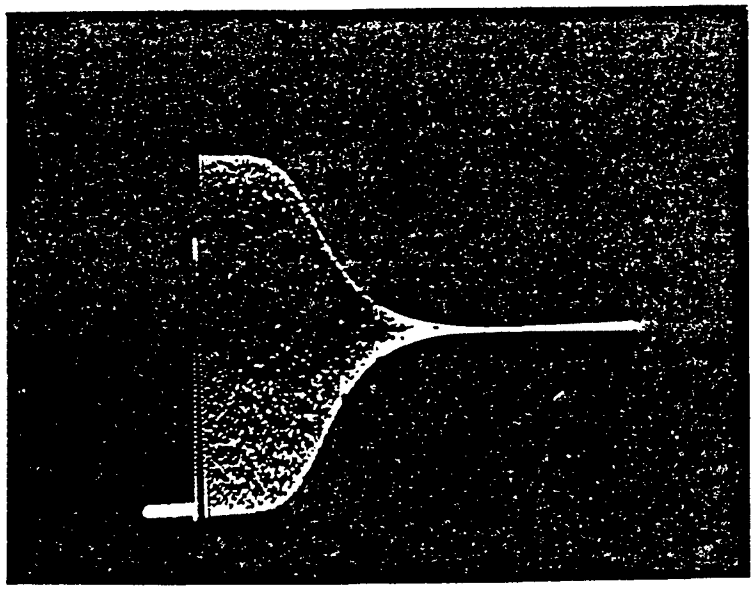

Fig.19 Experimental Frequency Response of Microprocessor-Based 3rd Order Butterworth Lowpass Filter $G_{LP}(z)$, (Example 1).

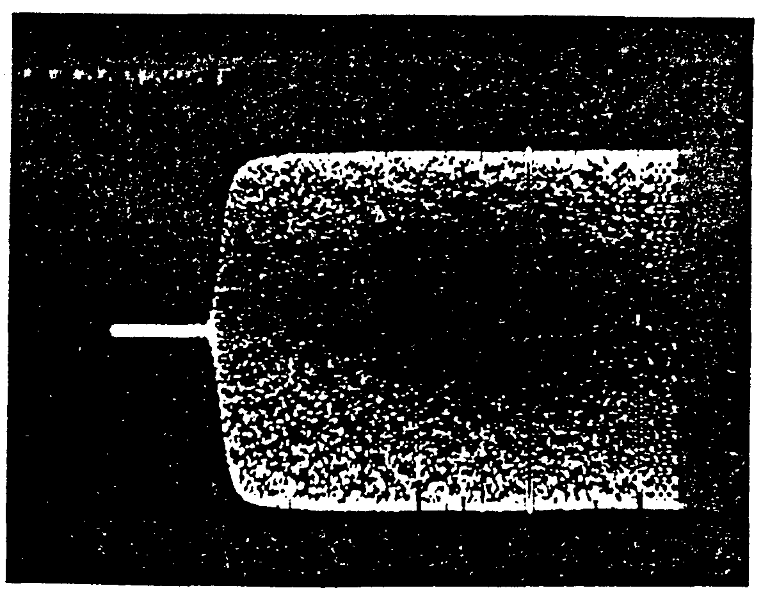

Fig.20 Experimental Frequency Response of Microprocessor-Based 3rd Order Butterworth Highpass Filter $G_{HP}(z)$ (Example 2)

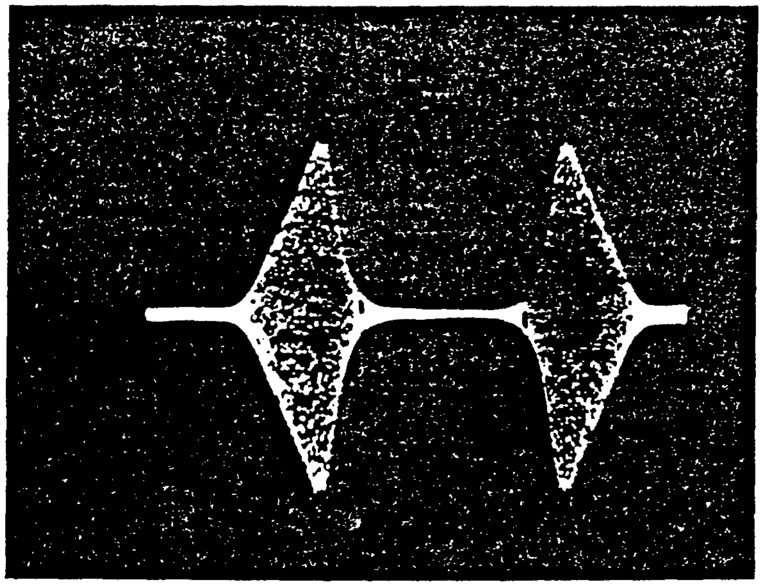

Fig.21 Experimental Frequency Response of Microprocessor-Based 6th Order Butterowrth Bandpass Filter $G_{BP}(z)$ (Example 3)

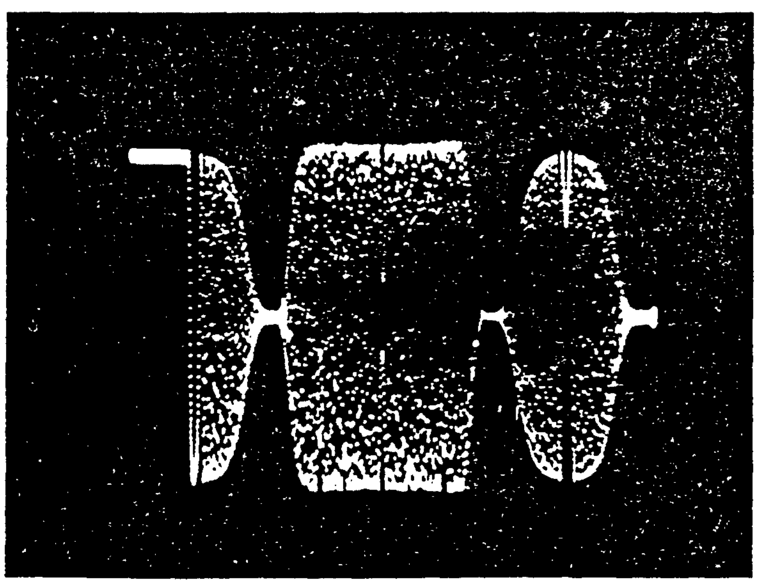

Fig.22 Experimental Frequency Response of Microprocessor-Based 6th Order Butterworth Bandstop Filter $G_{BS}(z)$ (Example 4)

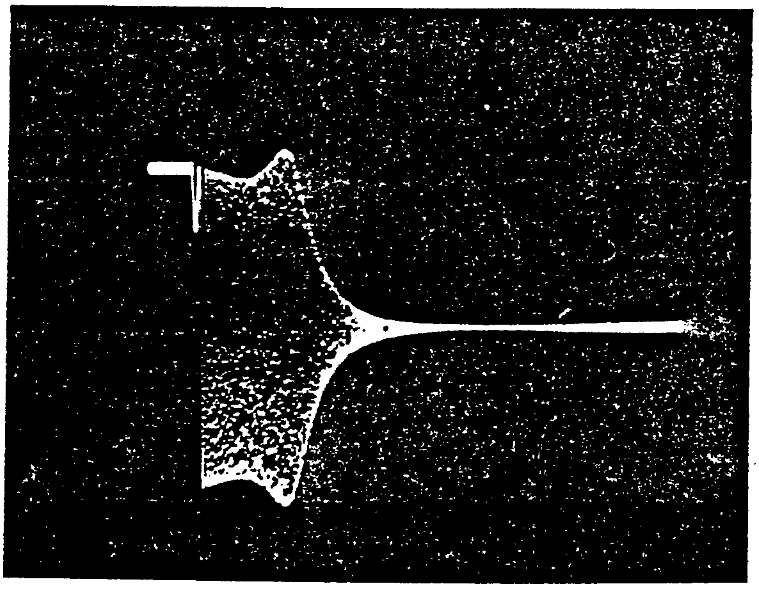

Fig.23 Experimental Frequency Response of Microprocessor-Based 3rd Order Chebychev Lowpass Filter (Example 5)

Table 2. Critical Frequencies of Theoretical and Microprocessor-Based Filters

Digital Filter		Sampling Frequency ω_s (Hz)	Cut-Off or Cut-In Frequency ω_{dc} (Hz)	Frequency at Attenuation = 0.1 $\omega_{0.1}$ (Hz)	Remarks
3rd Order Butterworth Lowpass	Theoretical	200	30	52	
	Experimental	200	27	49	
3rd Order Chebychev Lowpass	Theoretical	200	29	44	The cut-off rate is faster than that of the Butterworth filter.
	Experimental	200	27	45	
3rd Order Butterworth Highpass	Theoretical	200	10	5	
	Experimental	200	9.5	5	

Digital Filter		Sampling Frequency ω_s (Hz)	Midband Frequency ω_o (Hz)	First Aliasing Midband Freq. ω_1 (Hz)	Bandwidth BW (Hz)	Remarks
6th Order Butterworth Bandpass	Theoretical	100	25	75	7.5	$\omega_o/\omega_s = .25$
	Experimental	140	28	100	17	$\omega_o/\omega_s = .2$
6th Order Butterworth Bandstop	Theoretical	100	20	80	14	
	Experimental	104	16	78	16	

REFERENCES

[1] Krasnicki, E.J., "Comparison of analytical and experimental results for a semi-active vibration isolator," Shock & Vibration Bulletin, Part 4, pp. 69-76, Sept, 1980.

[2] Tomizuka, M., "Optimum linear preview control with application to vehicle suspension - revisited," Trans. ASME. J. of Dynamic Systems, Measurement, and Control, pp. 309-315, Sept, 1976.

[3] Woods, P., "Performance analysis of high-speed hydraulic suspension systems in multiple wheeled land transporters," Shock & Vibration Bulletin, No. 52, July, 1982.

[4] Margolis, D.L. and C.K. Schroeck, "Semi-active suspensions for military ground vehicles under off-road conditions," Technical Report, Mechanical Group, Lord Corporation, Erie, PA. Sept, 1981.

[5] Daigle B., "Application of digital filtering techniques to terrain roughness identification," Technical note, U.S. Army Automotive Command, Warren, MI 48090, 1981.

[6] Oppenheim, A.V. and Schafer R.W., Digital Signal Processing, Prentice-Hall Inc., New Jersey, 1975.

[7] Stretter S.A., Introduction to Discrete-Time Signal Processing, John Wiley & Sons, New York, 1976.

[8] Cadzow J.A., Discrete-Time Systems, Prentice Hall Inc., New Jersey, 1973.

[9] Haskell R.E. and G.A. Jackson, "Designing with microprocessors hardware and software," School of Engineering, Oakland University, Rochester, MI 48063, Feb., 1980.

THIS PAGE IS LEFT BLANK INTENTIONALLY.

APPENDIX A

SUMMARY OF ANALOG BUTTERWORTH FREQUENCY SELECTIVE FILTERS

A1. Low-Pass Filter $G_{LPN}(s)$ with Normalized Cut-Off Frequency ($\omega_{ac} = 1$):

$$G_{LPN}(s) = \frac{1}{(s - u_1)} \frac{1}{(s - u_2)} \cdots \frac{1}{(s - u_n)} \qquad \text{(A1)}$$

where[1] u_i, $i = 1, \ldots, n$, are the stable poles which lie on the unit circle in the s-plane as shown in Fig.A1.

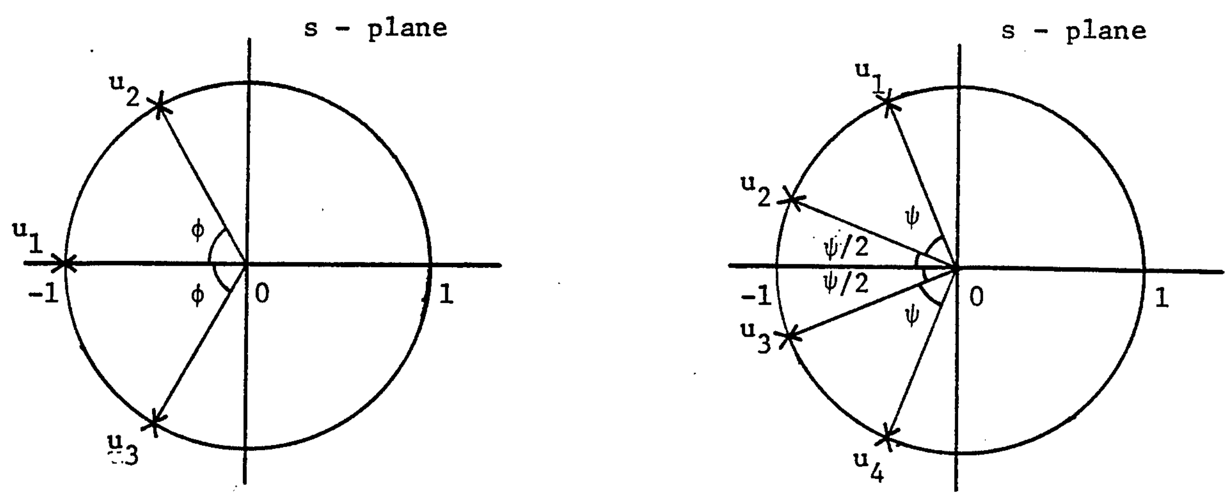

$\phi = \frac{\pi}{n}$ $\qquad\qquad$ $\psi = \frac{\pi}{n}$

n = odd (e.g., $n=3$) $\qquad\qquad$ n = even (e.g., $n=4$)

Fig. A1. Pole Locations of Normalized Butterworth Lowpass Filter

---

[1] We note that complex poles must occur in complex conjugate pairs in order for the filter to be physically realizable.

A2: Low-Pass Filter $G_{LP}(s)$ with Arbitrary Cut-Off Frequency ω_{ac}:

To translate $G_{LPN}(s)$ into $G_{LP}(s)$, one substitutes s/ω_{ac} for s in (A.1) and obtain

$$G_{LP}(s) = \frac{\omega_{ac}}{(s - \omega_{ac}u_1)} \frac{\omega_{ac}}{(s - \omega_{ac}u_2)} \cdots \frac{\omega_{ac}}{(s - \omega_{ac}u_n)} . \qquad (A.2)$$

A typical set of pole locations of $G_{LP}(s)$ is shown in Fig.A2.

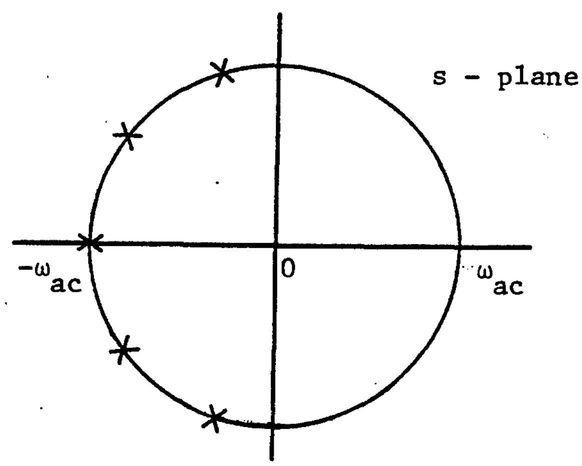

Fig. A2. Pole Locations of Butterworth Lowpass Filter with ω_{ac} (n = 5)

A3: High-Pass Filter $G_{HPN}(s)$ with Normalized Cut-In Frequency ($\omega_{ac} = 1$):

To translate $G_{LPN}(s)$ into $G_{HPN}(s)$, one substitutes 1/s for s in (A.1) and obtains

$$G_{HPN}(s) = \frac{s}{(1 - su_1)}\frac{s}{(1 - su_2)} \cdots \frac{s}{(1 - su_n)}$$

$$= \frac{(-1/u_1)s}{(s - 1/u_1)}\frac{(-1/u_2)s}{(s - 1/u_2)} \cdots \frac{(-1/u_n)s}{(s - 1/u_n)}$$

$$\doteq \frac{s}{(s - u_1)}\frac{s}{(s - u_2)} \cdots \frac{s}{(s - u_n)} \quad , \qquad \text{(A.3)}$$

where the last equality follows from the fact that $1/u_i = u_i^*$, $|u_i| = 1$ and u_i occur in complex conjugate pairs. A typical set of poles and zeroes for $G_{HPN}(s)$ is shown in Fig.A3.

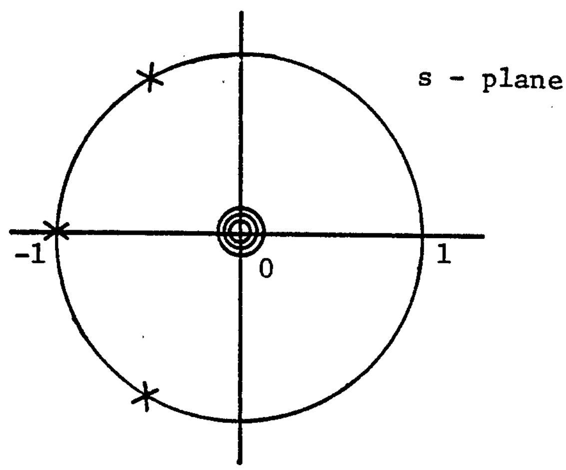

Fig. A3. Pole-Zero locations of Normalized Butterworth Highpass Filter. (n = 3)

A4: High-Pass Filter $G_{HP}(s)$ with Arbitrary Cut-In Frequency ω_{ac}:

To translate $G_{HPN}(s)$ to $G_{HP}(s)$, one substitutes s/ω_{ac} for s in (A.3) and obtains

$$G_{HP}(s) = \frac{s}{(s - \omega_{ac}u_1)} \frac{s}{(s - \omega_{ac}u_2)} \cdots \frac{s}{(s - \omega_{ac}u_n)} \quad ,$$

where a typical set of poles and zeroes for $G_{HP}(s)$ is shown in Fig.A4.

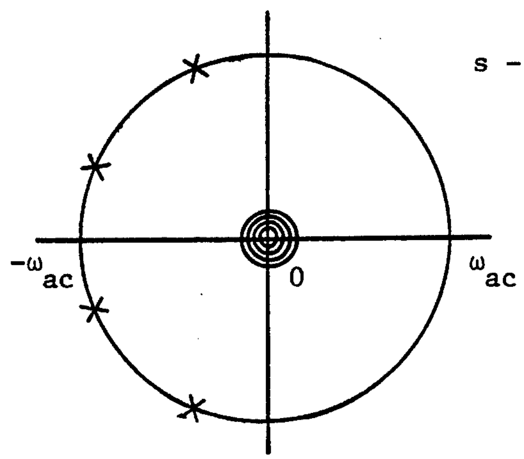

Fig. A4. Pole-Zero Locations of Butterworth Highpass Filter with ω_{ac}. (n = 4)

A5: Band-Pass Filter $G_{BP}(s)$ with Bandwidth BW and Midband Frequency ω_{ao}:

A high Q-factor will generally be assumed, i.e., $Q \triangleq \omega_{ao}/BW \geq 1$. To translate $G_{LPN}(s)$ to $G_{BP}(s)$, one substitutes

$\frac{1}{BW}\frac{s^2 + \omega_{ao}^2}{s}$ for s in (A.1) and obtains

$$G_{BP}(s) = \frac{BW.s}{(s^2 - BWu_1 s + \omega_{ao}^2)} \frac{BW.s}{(s^2 - BWu_2 s + \omega_{ao}^2)} \cdots \frac{BW.s}{(s^2 - BWu_n s + \omega_{ao}^2)}$$

$$\triangleq \frac{BW.s}{(s - p_1)(s - q_1)} \frac{BW.s}{(s - p_2)(s - q_2)} \cdots \frac{BW.s}{(s - p_n)(s - q_n)}$$

$$\cong \frac{BW.s}{(s - c_1)(s - c_1^*)} \frac{BW.s}{(s - c_2)(s - c_2^*)} \cdots \frac{BW.s}{(s - c_n)(s - c_n^*)}, \qquad \text{(A.5)}$$

where

$$p_i, q_i \triangleq \frac{BW}{2} u_i \pm \tfrac{1}{2}\sqrt{(BWu_i)^2 - 4\omega_{ao}^2}$$

which may be approximated by

$$c_i, c_i^* \triangleq \frac{BW}{2} u_i \pm j\omega_{ao}$$

for a high Q-factor. A typical pole-zero location of $G_{BP}(s)$ is shown in Fig. A5.

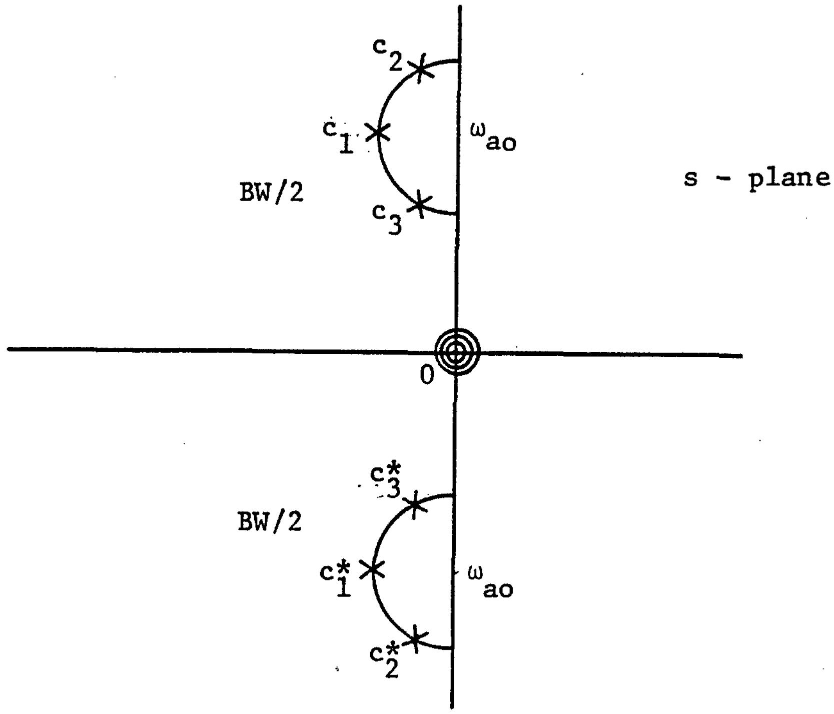

Fig. A5. Pole-Zero Locations of Butterworth Bandpass Filter with Bandwidth BW and Midband Frequency ω_{ao}.

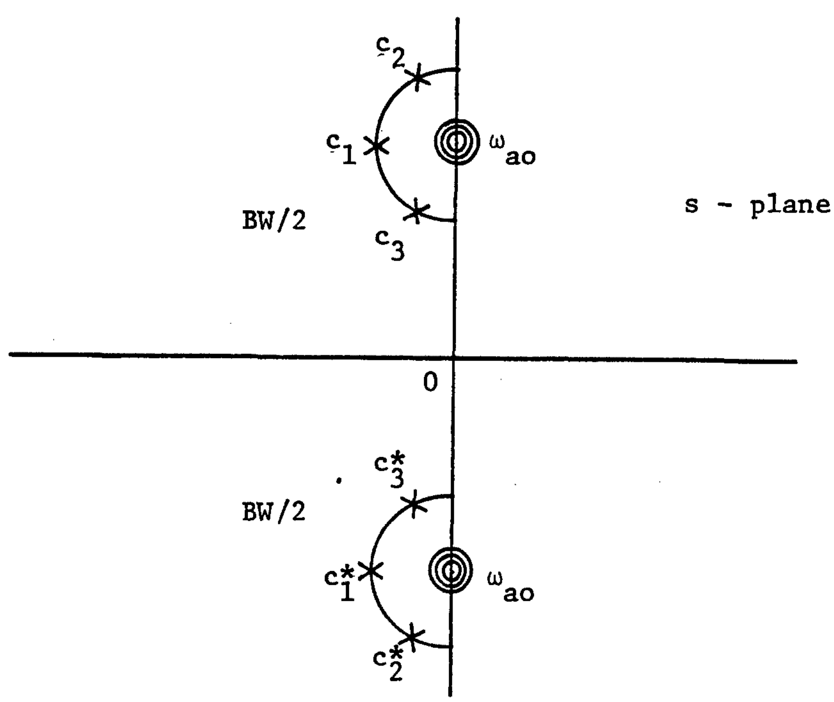

Fig. A6. Pole-Zero Locations of Butterworth Bandstop Filter with Bandwidth BW and Midband Frequency ω_{ao}.

A6: Band-Stop Filter $G_{BS}(s)$ with Bandwidth BW and Midband Frequency ω_{ao}:

A high Q-factor will similarly be assumed, i.e., $Q \triangleq \omega_{ao}/BW \geq 1$. To translate $G_{HPN}(s)$ to $G_{BS}(s)$, one substitutes

$BW \dfrac{s}{s^2 + \omega_{ao}^2}$ for s in (A.3) and obtains

$$G_{BS}(s) = \frac{(s^2 + \omega_{ao}^2)}{(s^2 - BWu_1 s + \omega_{ao}^2)} \frac{(s^2 + \omega_{ao}^2)}{(s^2 - BWu_2 s + \omega_{ao}^2)} \cdots \frac{(s^2 + \omega_{ao}^2)}{(s^2 - BWu_n s + \omega_{ao}^2)}$$

$$\simeq \frac{(s+j\omega_{ao})(s-j\omega_{ao})}{(s - c_1)(s - c_1^*)} \frac{(s+j\omega_{ao})(s-j\omega_{ao})}{(s - c_2)(s - c_2^*)} \cdots \frac{(s+j\omega_{ao})(s-j\omega_{ao})}{(s - c_n)(s - c_n^*)} \tag{A.6}$$

where c_i are as defined for (A5). A typical pole-zero location for $G_{BS}(s)$ is shown in Fig. A6.

THIS PAGE IS LEFT BLANK INTENTIONALLY.

APPENDIX B

MICROPROCESSOR PROGRAMS FOR DIGITAL FREQUENCY SELECTIVE FILTERS

MICROKIT 6800 DISK ASSEMBLER - VER 1

```
                        *
                        *
0008                    IDLTIM  EQU   X'08'
000A                    INITAD  EQU   X'0A'
000C                    DESTIN  EQU   X'0C'
000E                    XTEMP   EQU   X'0E'
0019                    CHNO    EQU   X'19'
                        *
0000                            ORG   X'A800'
A800  CEA900   MOVBLK   LDX   #X'A900'
A803  DF00              STX   X'00'
A805  CE0400            LDX   #X'0400'
A808  DF0C              STX   DESTIN
A80A  DE00              LDX   X'00'
A80C  DF0A              STX   INITAD
A80E  DE0A     MOVBYT   LDX   INITAD
A810  A600              LDAA  X'00',X
A812  08                INX
A813  DF0A              STX   INITAD
A815  DE0C              LDX   DESTIN
A817  A700              STAA  X'00',X
A819  8C07FF            CPX   #X'07FF
A81C  2705              BEQ   BEQ6
A81E  08                INX
A81F  DF0C              STX   DESTIN
A821  20EB              BRA   MOVBYT
A823  3F       BEQ6     SWI
                        *
```

```
A824 7F0015 MULT1  CLR  X'15'
A827 7F0016        CLR  X'16'
A82A 7F0017        CLR  X'17'
A82D CE0008        LDX  #X'0008'
A830 D610          LDAB X'10'
A832 770011 BNE11  ASR  X'11'
A835 760012        ROR  X'12'
A838 760013        ROR  X'13'
A83B 58            ASLB
A83C 2412          BCC  BCC11
A83E 9613          LDAA X'13'
A840 9B17          ADDA X'17'
A842 9717          STAA X'17'
A844 9612          LDAA X'12'
A846 9916          ADCA X'16'
A848 9716          STAA X'16'
A84A 9611          LDAA X'11'
A84C 9915          ADCA X'15'
A84E 9715          STAA X'15'
A850 09     BCC11  DEX
A851 26DF          BNE  BNE11
A853 39            RTS
            *
A854 A630   MUL    LDAA X'30',X
A856 9710          STAA X'10'
A858 A600          LDAA X'00',X
A85A 9711          STAA X'11'
A85C A610          LDAA X'10',X
A85E 9712          STAA X'12'
A860 A620          LDAA X'20',X
A862 9713          STAA X'13'
A864 DF0E          STX  XTEMP
A866 BDA824        JSR  MULT1
A869 DE0E          LDX  XTEMP
A86B 9615          LDAA X'15'
A86D A708          STAA X'08',X
A86F 9616          LDAA X'16'
A871 A718          STAA X'18',X
A873 9617          LDAA X'17'
A875 A728          STAA X'28',X
A877 9C0C          CPX  DESTIN
A879 2703          BEQ  OUT1
A87B 08            INX
A87C 20D6          BRA  MUL
A87E 39     OUT1   RTS
            *
A87F 7F002F SUM    CLR  X'2F'
A882 7F003F        CLR  X'3F'
A885 7F004F        CLR  X'4F'
A888 09            DEX
A889 08     BNE10  INX
A88A 964F          LDAA X'4F'
A88C AB20          ADDA X'20',X
A88E 974F          STAA X'4F'
A890 963F          LDAA X'3F'
A892 A910          ADCA X'10',X
A894 973F          STAA X'3F'
```

```
A896 962F          LDAA X'2F'
A898 A900          ADCA X'00',X
A89A 972F          STAA X'2F'
A89C 9C0C          CPX  DESTIN
A89E 26E9          BNE  BNE10
A8A0 39            RTS
              *
A8A1 6020   NEGATE NEG  X'20',X
A8A3 8600          LDAA #X'00'
A8A5 A210          SBCA X'10',X
A8A7 A710          STAA X'10',X
A8A9 8600          LDAA #X'00'
A8AB A200          SBCA X'00',X
A8AD A700          STAA X'00',X
A8AF 39            RTS
              *
A8B0 962F   TRANSF LDAA X'2F'
A8B2 A700          STAA X'00',X
A8B4 963F          LDAA X'3F'
A8B6 A710          STAA X'10',X
A8B8 964F          LDAA X'4F'
A8BA A720          STAA X'20',X
A8BC 39            RTS
              *
A8BD 7F8001 PIASU1 CLR  X'8001'
A8C0 7F8003        CLR  X'8003'
A8C3 7F8009        CLR  X'8009'
A8C6 7F800B        CLR  X'800B'
A8C9 86FF          LDAA #X'FF'
A8CB B78000        STAA X'8000'
A8CE B78002        STAA X'8002'
A8D1 4F            CLRA
A8D2 B78008        STAA X'8008'
A8D5 860F          LDAA #X'0F'
A8D7 B7800A        STAA X'800A'
A8DA 8634          LDAA #X'34'
A8DC B78001        STAA X'8001'
A8DF B78003        STAA X'8003'
A8E2 B78009        STAA X'8009'
A8E5 862C          LDAA #X'2C'
A8E7 B7800B        STAA X'800B'
A8EA 39            RTS
              *
A8EB 9710   MULT2  STAA X'10'
A8ED 7F0011        CLR  X'11'
A8F0 D712          STAB X'12'
A8F2 7F0013        CLR  X'13'
A8F5 BDA824        JSR  MULT1
A8F8 39            RTS
              *
A8F9 DE08   IDLE   LDX  IDLTIM
A8FB 09     IDL1   DEX
A8FC 26FD          BNE  IDL1
A8FE 39            RTS
              *
```

```
A8FF                     ORG  X'A900'
A900 8607        BIL01   LDAA #X'07'
A902 B7800A              STAA X'800A'
A905 CE002E              LDX  #X'002E'
A908 BDA8B0              JSR  TRANSF
A90B B68008              LDAA X'8008'
A90E 9725                STAA X'25'
A910 F6800A              LDAB X'800A'
A913 D735                STAB X'35'
                 *2
A915 CE0025              LDX  #X'0025'
A918 DF0C                STX  DESTIN
A91A BDA854              JSR  MUL
                 *3
A91D CE002E              LDX  #X'002E'
A920 DF0C                STX  DESTIN
A922 CE0028              LDX  #X'0028'
A925 BDA87F              JSR  SUM
                 *4
A928 962E                LDAA X'2E'
A92A 9722                STAA X'22'
A92C 963E                LDAA X'3E'
A92E 9732                STAA X'32'
                 *5
A930 CE0026              LDX  #X'0026'
A933 BDA8B0              JSR  TRANSF
A936 DF0C                STX  DESTIN
A938 BDA854              JSR  MUL
                 *6
A93B CE002D              LDX  #X'002D'
A93E BDA8B0              JSR  TRANSF
                 *
A941 39                  RTS
                 *
                 *
                 *
                 *8
A942 962F        HIL02   LDAA X'2F'
A944 D63F                LDAB X'3F'
A946 887F                EORA #X'7F'
A948 C8F0                EORB #X'F0'
A94A B78000              STAA X'8000'
A94D F78002              STAB X'8002'
                 *9
A950 CE0000              LDX  #X'0000'
A953 A621        UPYU    LDAA X'21',X
A955 E631                LDAB X'31',X
A957 A720                STAA X'20',X
A959 E730                STAB X'30',X
A95B 08                  INX
A95C 8C0005              CPX  #X'0005'
A95F 26F2                BNE  UPYU
                 *10
A961 CE0024              LDX  #X'0024'
A964 DF0C                STX  DESTIN
A966 CE0020              LDX  #X'0020'
A969 BDA854              JSR  MUL
```

```
                *11
A96C CE0029           LDX   #X'0029'
A96F BDA8A1           JSR   NEGATE
                *
A972 39               RTS
                *
                *
                *
A973 CE0010     CLRTIM LDX  #X'0010'
A976 6F1F       CCCCCC CLR  X'1F',X
A978 6F2F             CLR   X'2F',X
A97A 6F3F             CLR   X'3F',X
A97C 6F5F             CLR   X'5F',X
A97E 6F6F             CLR   X'6F',X
A980 6F7F             CLR   X'7F',X
A982 09               DEX
A983 26F1             BNE   CCCCCC
A985 CE0001           LDX   #X'0001'
A988 DF08             STX   IDLTIM
A98A 39               RTS
```

MICROKIT 6800 DISK ASSEMBLER - VER 1

```
                  *
                  *
                  *  LOW PASS FILTER 1
                  *
                  *
A98B 8E07FF LOPAS1 LDS   #X'07FF'
A98E BDA9AA        JSR   LODAT1
A991 BDA8BD GOLO   JSR   PIASU1
A994 BDA900 LP     JSR   HILO1
A997 CE002E        LDX   #X'002E'
A99A DF0C          STX   DESTIN
A99C CE002D        LDX   #X'002D'
A99F BDA87F        JSR   SUM
A9A2 BDA942        JSR   HILO2
A9A5 BDA8F9        JSR   IDLE
A9A8 20EA          BRA   LP
                  *
```

```
                 *
                 *
A9AA BDA973 LODAT1 JSR  CLRTIM
A9AD 861F          LDAA #X'1F'
A9AF 9750          STAA X'50'
A9B1 9753          STAA X'53'
A9B3 9754          STAA X'54'
A9B5 860A          LDAA #X'0A'
A9B7 9752          STAA X'52'
A9B9 9755          STAA X'55'
A9BB 869A          LDAA #X'9A'
A9BD 9751          STAA X'51'
A9BF 8619          LDAA #X'19'
A9C1 9756          STAA X'56'
A9C3 39            RTS
                 *
```

```
                    *
                    *
                    *   CHEBYCHEV LOWPASS FILTER
A9C4 8E07FF             LDS  #X'07FF'
A9C7 863E               LDAA #X'3E'
A9C9 9750               STAA X'50'
A9CB 86CC               LDAA #X'CC'
A9CD 9751               STAA X'51'
A9CF 8610               LDAA #X'10'
A9D1 9752               STAA X'52'
A9D3 9755               STAA X'55'
A9D5 8630               LDAA #X'30'
A9D7 9753               STAA X'53'
A9D9 9754               STAA X'54'
A9DB 86C6               LDAA #X'C6'
A9DD 9756               STAA X'56'
A9DF 2080               BRA  GOLD
                    *
```

```
                    *
                    *
                    *  HIGH PASS FILTER 1
                    *
A9E1 8E07FF HIPAS1 LDS  #X'07FF'
A9E4 BDAACF        JSR  HIDAT1
A9E7 BDA8BD GOHI   JSR  PIASU1
A9EA BDA930 HP     JSR  HILO1     STEPS 1 TO 6
A9ED CE002E        LDX  #X'002E'
A9F0 DF0C          STX  DESTIN    STEP 7
A9F2 CE002C        LDX  #X'002C'
A9F5 BDA8B0        JSR  TRANSF
A9F8 BDA87F        JSR  SUM
A9FB BDA942        JSR  HILO2     STEP2 8 TO 11
A9FE CE002A        LDX  #X'002A'
AA01 BDA8A1        JSR  NEGATE
AA04 CE002C        LDX  #X'002C'
AA07 BDA8A1        JSR  NEGATE
AA0A BDA8F9        JSR  IDLE      STEP 12
AA0D 20DB          BRA  HP
                   *
```

```
                        *
                        *
AA0F BDA973  HIDAT1  JSR   CLRTIM
AA12 8639            LDAA  #X'39'
AA14 9750            STAA  X'50'
AA16 86D0            LDAA  #X'D0'
AA18 9751            STAA  X'51'
AA1A 864F            LDAA  #X'4F'
AA1C 9752            STAA  X'52'
AA1E 9755            STAA  X'55'
AA20 86EC            LDAA  #X'EC'
AA22 9753            STAA  X'53'
AA24 9754            STAA  X'54'
AA26 8660            LDAA  #X'60'
AA28 9756            STAA  X'56'
AA2A 39              RTS
                        **
                        *
```

```
                  *
                  * SUBROUTINES FOR BANDPASS & BANDSTOP
                  *
AA2B 8607         BPBS1  LDAA  #X'07'
AA2D B7800A              STAA  X'800A'
AA30 9624                LDAA  X'24'
AA32 D634                LDAB  X'34'
AA34 972C                STAA  X'2C'
AA36 D73C                STAB  X'3C'
AA38 9644                LDAA  X'44'
AA3A 974C                STAA  X'4C'
AA3C CE002C              LDX   #X'002C'
AA3F BDA8A1              JSR   NEGATE
AA42 39                  RTS
                  *
                  *
                  *
AA43 DF0C         BPBS2  STX   DESTIN      STEP 3
AA45 CE0068              LDX   #X'0068'
AA48 BDA87F              JSR   SUM
AA4B CE002E              LDX   #X'002E'
AA4E BDA8B0              JSR   TRANSF
                  *                        STEP 4
AA51 DF0C                STX   DESTIN
AA53 CE0028              LDX   #X'0028'
AA56 BDA87F              JSR   SUM
                  *                        STEP 5
AA59 CE0026              LDX   #X'0026'
AA5C BDA8B0              JSR   TRANSF
AA5F DF0C                STX   DESTIN
AA61 BDA854              JSR   MUL
AA64 CE002E              LDX   #X'002E'
AA67 DF0C                STX   DESTIN
AA69 CE002D              LDX   #X'002D'
AA6C BDA8B0              JSR   TRANSF
AA6F BDA87F              JSR   SUM
                  *                        STEP 6
AA72 962F                LDAA  X'2F'
AA74 D63F                LDAB  X'3F'
AA76 882F                EORA  #X'2F'
AA78 C8F0                EORB  #X'F0'
AA7A B78000              STAA  X'8000'
AA7D F78002              STAB  X'8002'
                  *                        STEP 7
AA80 CE0000              LDX   #X'0000'
AA83 A621         YUP    LDAA  X'21',X
AA85 E631                LDAB  X'31',X
AA87 A720                STAA  X'20',X
AA89 E730                STAB  X'30',X
AA8B A641                LDAA  X'41',X
AA8D A740                STAA  X'40',X
AA8F 08                  INX
AA90 8C0005              CPX   #X'0005'
AA93 26EE                BNE   YUP
AA95 CE0025              LDX   #X'0025'
AA98 BDA8B0              JSR   TRANSF
                  *                        STEP 8
```

```
AA9B CE0023      LDX  #X'0023'
AA9E DF0C        STX  DESTIN
AAA0 CE0020      LDX  #X'0020'
AAA3 BDA854      JSR  MUL
AAA6 CE0025      LDX  #X'0025'
AAA9 DF0C        STX  DESTIN
AAAB BDA854      JSR  MUL
              *                 STEP 9
AAAE CE0028      LDX  #X'0028'
AAB1 BDA8A1      JSR  NEGATE
AAB4 CE002A      LDX  #X'002A'
AAB7 BDA8A1      JSR  NEGATE
              *
AABA 39          RTS
```

```
                    ***
                    **
                    *
                    *   BANDPASS FILTER 1
                    *
                    **
                    ***
AAB8 8E07FF  BPASS1 LDS   #X'07FF'
AABE BDAB14         JSR   BPDAT1
AAC1 BDA8BD  GOBP   JSR   PIASU1
                    *                     STEP1
AAC4 BDAA2B  BP     JSR   BPBS1
AAC7 B6800B         LDAA  X'800B'
AACA 9763           STAA  X'63'
AACC F6800A         LDAB  X'800A'
AACF D773           STAB  X'73'
                    *                     STEP2
AAD1 CE0063         LDX   #X'0063'
AAD4 DF0C           STX   DESTIN
AAD6 BDA854         JSR   MUL
                    *                     STEP3
AAD9 CE006B         LDX   #X'006B'
AADC BDAA43         JSR   BPBS2
                    *                     STEP10
AADF CE0000         LDX   #X'0000'
AAE2 A664    UPUBP  LDAA  X'64',X
AAE4 A760           STAA  X'60',X
AAE6 A661           LDAA  X'61',X
AAE8 A764           STAA  X'64',X
AAEA E674           LDAB  X'74',X
AAEC E770           STAB  X'70',X
AAEE E671           LDAB  X'71',X
AAF0 E774           STAB  X'74',X
AAF2 08             INX
AAF3 8C0003         CPX   #X'0003'
AAF6 26EA           BNE   UPUBP
                    *                     STEP11
AAF8 CE0062         LDX   #X'0062'
AAFB DF0C           STX   DESTIN
AAFD CE0060         LDX   #X'0060'
AB00 BDA854         JSR   MUL
                    *                     STEP 12
AB03 CE0068         LDX   #X'0068'
AB06 BDA8A1         JSR   NEGATE
AB09 CE006A         LDX   #X'006A'
AB0C BDA8A1         JSR   NEGATE
                    *                     STEP 13
AB0F BDA8F9         JSR   IDLE
AB12 20B0           BRA   BP
                    *
```

```
                  *
                  *
AB14 BDA973 BFDAT1 JSR  CLRTIM
AB17 8615          LDAA #X'15'
AB19 9750          STAA X'50'
AB1B 8634          LDAA #X'34'
AB1D 9751          STAA X'51'
AB1F 8691          LDAA #X'91'
AB21 9752          STAA X'52'
AB23 86BE          LDAA #X'BE'
AB25 9753          STAA X'53'
AB27 86FF          LDAA #X'FF'
AB29 9754          STAA X'54'
AB2B 86A9          LDAA #X'A9'
AB2D 9755          STAA X'55'
AB2F 86C3          LDAA #X'C3'
AB31 9756          STAA X'56'
AB33 8606          LDAA #X'06'
AB35 9790          STAA X'90'
AB37 9793          STAA X'93'
AB39 8612          LDAA #X'12'
AB3B 9791          STAA X'91'
AB3D 9792          STAA X'92'
AB3F 39            RTS
                  *
                  *
                  *
```

```
                 ***
                 **
                 *
                 * BANDSTOP FILTER 1
                 *
                 **
                 ***
AB40 8E07FF  BSTOP1 LDS   #X'07FF'
AB43 BDA697         JSR   BSDAT1
AB46 BDA8BD  GOBS   JSR   PIASU1
AB49 BDAA2B  BS     JSR   BPBS1
AB4C B68008         LDAA  X'8008'
AB4F 9766           STAA  X'66'
AB51 F6800A         LDAB  X'800A'
AB54 D776           STAB  X'76'
             *                      STEP 2
AB56 CE0066         LDX   #X'0066'
AB59 DF0C           STX   DESTIN
AB5B BDA854         JSR   MUL
             *                      STEP 3
AB5E CE006E         LDX   #X'006E'
AB61 BDAA43         JSR   BPBS2
             *                      STEP 10
AB64 CE0000         LDX   #X'0000'
AB67 A661    UPUBS  LDAA  X'61',X
AB69 A760           STAA  X'60',X
AB6B E671           LDAB  X'71',X
AB6D E770           STAB  X'70',X
AB6F 08             INX
AB70 8C0006         CPX   #X'0006'
AB73 26F2           BNE   UPUBS
             *                      STEP11
AB75 CE0065         LDX   #X'0065'
AB78 DF0C           STX   DESTIN
AB7A CE0060         LDX   #X'0060'
AB7D BDA854         JSR   MUL
             *                      STEP 14
AB80 CE0069         LDX   #X'0069'
AB83 BDA8A1         JSR   NEGATE
AB86 CE006B         LDX   #X'006B'
AB89 BDA8A1         JSR   NEGATE
AB8C CE006D         LDX   #X'006D'
AB8F BDA8A1         JSR   NEGATE
             *                      STEP 15
AB92 BDA8F9         JSR   IDLE
             *
AB95 20B2           BRA   BS
             *
```

```
                  *
                  *
AB97 BDA973 BSDAT1 JSR  CLRTIM
AB9A 8615          LDAA #X'15'
AB9C 9750          STAA X'50'
AB9E 8634          LDAA #X'34'
ABA0 9751          STAA X'51'
ABA2 8691          LDAA #X'91'
ABA4 9752          STAA X'52'
ABA6 86BE          LDAA #X'BE'
ABA8 9753          STAA X'53'
ABAA 86A9          LDAA #X'A9'
ABAC 9755          STAA X'55'
ABAE 86FF          LDAA #X'FF'
ABB0 9754          STAA X'54'
ABB2 86C3          LDAA #X'C3'
ABB4 9756          STAA X'56'
ABB6 8637          LDAA #X'37'
ABB8 9790          STAA X'90'
ABBA 9796          STAA X'96'
ABBC 8665          LDAA #X'65'
ABBE 9791          STAA X'91'
ABC0 9795          STAA X'95'
ABC2 86E3          LDAA #X'E3'
ABC4 9792          STAA X'92'
ABC6 9794          STAA X'94'
ABC8 8606          LDAA #X'06'
ABCA 9793          STAA X'93'
ABCC 39            RTS
                 **
                 *
                 **
ABCD               END  MOVBLK
```

MICROKIT 6800 DISK ASSEMBLER — VER 1.0

A	0000	B	0000	X	0000	IDLTIM	0008
INITAD	000A	DESTIN	000C	XTEMP	000E	CHNO	0019
MOVBLK	A800	MOVBYT	A80E	BEQ6	A823	MULT1	A824
BNE11	A832	BCC11	A850	MUL	A854	OUT1	A87E
SUM	A87F	BNE10	A889	NEGATE	A8A1	TRANSF	A8B0
PIASU1	A8BD	MULT2	A8EB	IDLE	A8F9	IDL1	A8FB
HILO1	A900	HILO2	A942	UPYU	A953	CLRTIM	A973
CCCCCC	A976	LOPAS1	A9BB	GOLO	A991	LP	A994
LODAT1	A9AA	HIPAS1	A9E1	GOHI	A9E7	HP	A9EA
HIDAT1	AA0F	BPBS1	AA2B	BPBS2	AA43	YUP	AA03
BPASS1	AABB	GOBP	AAC1	BP	AAC4	UPUBP	AAE2
BPDAT1	AB14	BSTOP1	AB40	GOBS	AB46	BS	AB49
UPUBS	AB67	BSDAT1	AB97	CHEBY	A9C4		

THIS PAGE IS LEFT BLANK INTENTIONALLY.

APPENDIX C

DERIVATION OF DIGITAL FILTERS

C.1. Derivation of Eq. (14)

From (A.2),

$$G_{LP}(s) = \frac{\omega_{ac}}{(s-\omega_{ac}u_1)} \quad \frac{\omega_{ac}}{(s-\omega_{ac}u_2)} \cdots \frac{\omega_{ac}}{(s-\omega_{ac}u_n)} \quad .$$

Using the substitution in (14), one obtains

$$G_{LP}(z) = G_{LP}(s)\Big|_{s = \frac{\omega_{ac}}{R} \frac{z-1}{z+1}}$$

$$= \frac{\omega_{ac}}{\left(\frac{\omega_{ac}}{R}\frac{z-1}{z+1} - \omega_{ac}u_1\right)} \cdots \frac{\omega_{ac}}{\left(\frac{\omega_{ac}}{R}\frac{z-1}{z+1} - \omega_{ac}u_n\right)}$$

$$= \frac{R(z+1)}{[z-1 - Ru_1(z+1)]} \cdots \frac{R(z+1)}{[z-1 - Ru_n(z+1)]}$$

$$= \frac{R^n}{(1-u_1R)\ldots(1-u_nR)} \quad \frac{(z+1)^n}{\left(z - \frac{1+u_1R}{1-u_1R}\right)\ldots\left(z - \frac{1+u_nR}{1-u_nR}\right)}$$

$$\triangleq K \frac{(z+1)^n}{(z-p_1)\ldots(z-p_n)}$$

(c.f. Section 2.2)

C.2. Derivation of Eq. (21)

From (A.3),

$$G_{HP}(s) = \frac{s}{(s-\omega_{ac}u_1)} \quad \frac{s}{(s-\omega_{ac}u_2)} \cdots \frac{s}{(s-\omega_{ac}u_n)} \quad .$$

Using the substitution in (21), one obtains

$$G_{HP}(z) = G_{HP}(s)\Big|_{s=\frac{\omega_{ac}}{R}\frac{z-1}{z+1}}$$

$$= \frac{\frac{\omega_{ac}}{R}\frac{z-1}{z+1}}{(\frac{\omega_{ac}}{R}\frac{z-1}{z+1} - \omega_{ac}u_1)} \cdots \frac{\frac{\omega_{ac}}{R}\frac{z-1}{z+1}}{(\frac{\omega_{ac}}{R}\frac{z-1}{z+1} - \omega_{ac}u_n)}$$

$$= \frac{z-1}{[z-1 - u_1R(z+1)]} \cdots \frac{z-1}{[z-1 - u_nR(z+1)]}$$

$$= \frac{1}{(1-u_1R)\dots(1-u_nR)} \frac{(z-1)^n}{(z - \frac{1+u_1R}{1-u_1R}) \cdots (z - \frac{1+u_nR}{1-u_nR})}$$

$$\triangleq K \frac{(z-1)^n}{(z-p_1)\dots(z-p_n)}$$

(c.f. Section 2.3).

C.3. Derivation of Eq. (28)

From (A.5)

$$G_{BP}(s) \simeq \frac{BW.s}{(s-c_1)(s-c_1^*)} \frac{BW.s}{(s-c_2)(s-c_2^*)} \cdots \frac{BW.s}{(s-c_n)(s-c_n^*)}$$

Using the substitution in (28), one obtains

$$G_{BP}(2) = G_{BP}(s)\Big|_{s=\frac{2}{\tau}\frac{z-1}{z+1}}$$

$$= \frac{BW\frac{2}{\tau}\frac{z-1}{z+1}}{(\frac{2}{\tau}\frac{z-1}{z+1} - c_1)(\frac{2}{\tau}\frac{z-1}{z+1} - c_1^*)} \cdots \frac{BW\frac{2}{\tau}\frac{z-1}{z+1}}{(\frac{2}{\tau}\frac{z-1}{z+1} - c_n)(\frac{2}{\tau}\frac{z-1}{z+1} - c_n^*)}$$

$$= \frac{BW\frac{2}{\tau}(z-1)(z+1)}{(\frac{2}{\tau} - c_1)(\frac{2}{\tau} - c_1^*)[z - \frac{(\frac{2}{\tau}+c_1)}{(\frac{2}{\tau}-c_1)}][z - \frac{\frac{2}{\tau}-c_1^*)}{(\frac{2}{\tau}-c_1^*)}]} \cdots \frac{BW\frac{2}{\tau}(z-1)(z+1)}{(\frac{2}{\tau}-c_n)(\frac{2}{\tau}-c_n^*)[z - \frac{(\frac{2}{\tau}+c_n)}{(\frac{2}{\tau}-c_n)}][z - \frac{(\frac{2}{\tau}\ c_n^*)}{(\frac{2}{\tau}-c_n^*)}]}$$

$$\triangleq K \frac{(z-1)^n(z+1)^n}{(z-p_1)(z-p_1^*)\ldots(z-p_n)(z-p_n^*)}$$

(c.f. Section 2.4).

C.4. Derivation of Eq. (36)

From (A.6),

$$G_{BS}(s) \approx \frac{(s+j\omega_{ao})(s-j\omega_{ao})}{(s-c_1)(s-c_1^*)} \cdots \frac{(s+j\omega_{ao})(s-j\omega_{ao})}{(s-c_n)(s-c_n^*)} .$$

Using the substitution in (36), we obtain

$$G_{BS}(z) = G_{BS}(s) \Big|_{s = \frac{2}{\tau}\frac{z-1}{z+1}}$$

$$= \frac{(\frac{2}{\tau}\frac{z-1}{z+1} + j\omega_{ao})(\frac{2}{\tau}\frac{z-1}{z+1} - j\omega_{ao})}{(\frac{2}{\tau}\frac{z-1}{z+1} - c_1)(\frac{2}{\tau}\frac{z-1}{z+1} - c_1^*)} \cdots$$

$$= \frac{(\frac{2}{\tau}+j\omega_{ao})(\frac{2}{\tau}-j\omega_{ao})\left[z-\left(\frac{\frac{2}{\tau}-j\omega_{ao}}{\frac{2}{\tau}+j\omega_{ao}}\right)\right]\left[z-\left(\frac{\frac{2}{\tau}+j\omega_{ao}}{\frac{2}{\tau}-j\omega_{ao}}\right)\right]}{(\frac{2}{\tau}-c_1)(\frac{2}{\tau}-c_1^*)\left[z-\left(\frac{\frac{2}{\tau}+c_1}{\frac{2}{\tau}-c_1}\right)\right]\left[z-\left(\frac{\frac{2}{\tau}+c_1^*}{\frac{2}{\tau}-c_1^*}\right)\right]} \cdots$$

$$\triangleq K \frac{[z-z_0]^n[z-z_0^{-1}]^n}{\prod_{i=1}^{n}(z-p_i)(z-p_i^*)}$$

(c.f. Section 2.5).

7102A

THIS PAGE IS LEFT BLANK INTENTIONALLY.

DISTRIBUTION LIST
(As of 1 January 1983)

Please notify USATACOM, DRSTA-ZSA, Warren, Michigan 48090, of corrections and/or changes in address.

Superintendent
US Military Academy
ATTN: Dept. of Engineering
Course Director for
Autmv Engineering
West Point, NY 10996 . . . . . (01)

Commander
US Army Logistic Center
ATTN: ATCL-CC
Mr. J. McClure
Ft. Lee, VA 23801 . . . . . (01)

US Army Research Office
P.O. Box 12211
ATTN: Dr. David Mann
Research Triangle Park, NC 27709 (01)

HQDA
Office of Dep Chief of Staff for Rsch
Dev & Acquisition
ATTN: Dir of Army Research, ARZ-A
Dr. Lasser
Washington, DC 20310 . . . . . (01)

Commander
US Army Mobility Equipment
R&D Command
ATTN: DRDME-RT
Ft. Belvoir, VA 220606 . . . . . (01)

Director
US Army Corps of Engineers
Waterways Experiment Station
P.O. Box 631
ATTN: Mr. Nuttall
Vicksburg, MS 39180 . . . . . (01)

Director
US Army Cold Regions Research
& Engineering Lab
P.O. Box 282
ATTN: Dr. Liston
Library
Hanover, NH 03755 . . . . . (01)

Commander
US Army Test & Evaluation Command
Aberdeen Proving Grounds
ATTN: AMSTE-BB
AMSTE-TA
APG, MD 21005 . . . . . (02)

Commander
Rock Island Arsenal
ATTN: SARRI-LR
Rock Island, IL 61201 . . . . (02)

Commander
US Army Yuma Proving Ground
ATTN: STEYP-RPT
STEYP-TE
Yuma, AZ 85364 . . . . . (02)

Director
US Army Human Engineering Lab
Aberdeen Proving Grounds
ATTN: Mr. Eckles
APG, MD 21005 . . . . . (01)

Director
US Army Ballistic Research Lab
Aberdeen Proving Grounds
APG, MD 21005 . . . . . (01)

Director
US Army Material Systems Analysis
Agency
Aberdeen Proving Grounds
ATTN: Mr. Harold Burke
APG, MD 21005 . . . . . (01)

Director
National Tillage Machinery Lab
Box 792
Auburn, AL 36830 . . . . . (01)

Director
USDA Forest Service Equipment
Development Center
444 EAst Bonita Avenue
San Dimes, CA 91773 . . . . . (01)

Director
Keweenaw Research Center
Michigan Technological Univ.
Houghton, MI 49931 . . . . . (01)

Engineering Society Library
345 East 47th Street
New York, NY 10017 . . . . . (01)

Dr. M. C. Bekker
224 East Islav Drive
Santa Barbara, CA 93101. . . . . (01)

Mr. R. S. Wismer
Deere & Company
Engineering Research
3300 River Drive
Moline, IL 61265 . . . . . (01)

The University of Iowa
ATTN: Dr. E. Haug
Iowa City, IA 52242 . . . . . (01)

Stevens Institute of Technology
Castle Point Station
ATTN: Irwin Kamm
Hoboken, NJ 07030 . . . . . (02)

SFM
FOA 2
Box 27322
S-102 54 STOCKHOLM
Sweden . . . . . (02)

Mr. Hedwig
RU III/6
Ministry of Defense
5300 Bonn, Germany . . . . . (02)